2010

Synthesis and Characterization of a Novel Amphiphilic Core-Corona Hyperbranched Polymer, composed of EHMO and EHMOpeg, for drug delivery.

Khushboo Sharma
Virginia Commonwealth University

School of Engineering
Virginia Commonwealth University

This is to certify that the thesis prepared by Khushboo Sharma entitled SYNTHESIS AND CHARACTERIZATION OF A NOVEL AMPHIPHILIC CORE-CORONA HYPERBRANCHED POLYMER, COMPOSED OF EHMO AND $EHMO_{PEG}$, FOR DRUG DELIVERY has been approved by her committee as satisfactory completion of the thesis requirement for the degree of Masters of Science in Biomedical Engineering.

Dr. Hu Yang, Ph.D., Thesis Director, School of Engineering

Dr. Kenneth J. Wynne, Ph.D., School of Engineering

Dr. Gary L. Bowlin, Ph.D., School of Engineering

Dr. Gerald E. Miller, Ph.D., Department Chair, School of Engineering

Dr. Rosalyn S. Hobson, Ph.D., Associate Dean of Graduate Studies, School of Engineering

Dr. Russell D. Jamison, Ph.D., Dean, School of Engineering

Dr. F. Douglas Boudinot, Dean of the School of Graduate Studies

July 22, 2010.

SYNTHESIS AND CHARACTERIZATION OF A NOVEL AMPHIPHILIC CORE-CORONA HYPERBRANCHED POLYMER, COMPOSED OF EHMO AND $EHMO_{PEG}$, FOR DRUG DELIVERY

A thesis submitted in partial fulfillment of the requirements for the degree of Masters of Science in Biomedical Engineering at Virginia Commonwealth University.

by

KHUSHBOO SHARMA
B.E., ICFAI University, India, 2008

Director: DR. HU YANG
ASSISTANT PROFESSOR, BIOMEDICAL ENGINEERING

Virginia Commonwealth University
Richmond, Virginia
August 2010

Acknowledgement

I would like to thank my research advisor Dr. Hu Yang for his unconditional support, guidance and innovative ideas during the course of my master's education. He has been a constant source of inspiration. I am extremely lucky and glad to have him as my advisor. I would also like to thank the members of my thesis committee, Dr. Kenneth J. Wynne and Dr. Gary Bowlin for reviewing and evaluating my research. I am especially thankful to Dr. Kenneth J. Wynne for guiding me at every step and allowing me to work in his lab and use his equipment to carry out polymer synthesis and characterization. I would like to thank each and every member of Dr. Wynne's group, for their patience and time. I am indebted to Souvik Chakrabarty for helping me right from the beginning till the end. I am grateful to him for his helpful insights and invaluable suggestions throughout. I am thankful to Alpana Dongargaonkar, Olga Zolotarskaya, Quan Yuan, Christopher Holden and Kaavya Vidwans for their support and assistance throughout my matriculation at Virginia Commonwealth University. Being with all of them was a great learning experience and they all made the lab a fun place. Sincere thanks to School of Engineering, VCU for giving me this wonderful opportunity to study here.

I am extremely grateful to my roommates and friends, Alpana, Aditi, Yamini, and Sudarshana for their love and emotional support. I dedicate this achievement to my

family and my mentor who encouraged me throughout; with out their support I would not have been able to reach here.

Table of Contents

Page

Acknowledgements i

List of Tables vi

List of Figures vii

Chapter:

1 Introduction 1

2 Background 3

2.1 A brief history of branched polymers 3

2.2 Dendritic polymers 3

2.3 Dendrigraft polymers 6

2.4 Hyperbranched polymers 7

2.4.1 Methods of synthesis of hyperbranched polymers 8

2.4.1.1 Polycondensation of AB_x monomers 8
2.4.1.2 Proton transfer polymerization 9
2.4.1.3 Ring opening polymerization 10

2.4.2 Degree of branching 11

2.4.3 Properties of hyperbranched polymers 12

2.5 Drug delivery 13

3 Materials and methods 15

3.1 Materials 15

3.2 Equipment 16

3.3 Synthesis 17

3.3.1 Monomer synthesis 17
3.3.2 Synthesis of polymer 18
3.3.3 Preparation of polymeric particles 20

3.4 Characterization 21

3.4.1 Nuclear magnetic resonance spectroscopy 21
3.4.2 Differential scanning calorimetry 21
3.4.3 Fourier transform infrared spectroscopy 22
3.4.4 Dynamic light scattering 22
3.4.5 Scanning electron microscopy 24

3.5 Drug loading and encapsulation studies 25

3.6 Cytotoxicity studies 26

3.7 Drug release studies 26

4 Results and Discussion 29

4.1 Preparation and characterization of $EHMO_{PEG}$ and

poly(EHMO- $EHMO_{PEG}$) 29

4.2 Degree of branching 36

4.3 Mechanisms governing the reaction 39

4.4 Fourier transform infrared spectroscopy 42

4.5 Differential scanning calorimetry 45

4.6 Molecular weight determination 51

4.7 Preparation of polymeric particles 51

4.8 Cytotoxicity studies 60

5 Drug release kinetics 65

5.1 Loading and encapsulation studies 69

5.2 Drug release study 70

5.3 Cellular assay 72

5.4 Conclusions 73

5 Summary and future work 74

References 75

Vita 79

List of Tables and Schemes

Page

Table 1: List of materials used. 15

Table 2: List of equipments and machines used. 16

Table 3: NMR shifts for commonly used solvents 21

Table 4: ^{1}H-NMR shifts for monomer characterization. 29

Table 5: ^{1}H-NMR shifts for polymer characterization 30

Table 6: ^{13}C- NMR shifts for polymer characteriozation. 30

Table 7: Degree of branching of various polymeric ratios 36

Table 8: Glass transition temperatures 45

Table 9: Molecular weights determined from DLS 51

Table 10: Particle size determined using DLS and SEM 52

Table 11: Loading efficiencies 69

Table 12: Encapsulation efficiencies 70

Scheme 1: PEGylated monomer synthesis 18

Scheme 2: Polymer synthesis 20

Scheme 3: Mechanism of polymer synthesis 39

List of Figures

Page

Figure 1: Divergent method of dendrimer synthesis 5

Figure 2: Convergent method of dendrimer synthesis 6

Figure 3: Synthesis of denrigraft polymer 7

Figure 4: Self Polycondensation of AB_2 monomers 9

Figure 5: Self Poly-condensation vinyl polymerization. 9

Figure 6: Proton transfer polymerization 10

Figure 7: Ring opening polymerization 11

Figure 8: Degree of branching 12

Figure 9: Working principle of DLS 23

Figure 10: Working principle of SEM 25

Figure 11: UV- Vis scan of CPT (1mg/ml) 28

Figure 12: Standard calibration curve for CPT at 360 nm 28

Figure 13: ^{1}H-NMR spectra of monomers 31

Figure 14: NMR spectra of polymers 32

Figure 15: NMR spectra for degree of branching 37

Figure 16: FT-IR plots for different polymeric ratios 43

Figure 17: DSC curves 46

Figure 18: SEM images of blank polymeric particles 54

Figure 19: Comparison study between blank and drug loaded particles 56

Figure 20: Cytotoxicity studies 60

Figure 21: Microscopic images of cytotoxicity studies 61

Figure 22: Drug release kinetics 71

Figure 23: Cellular assay 72

Abstract

SYNTHESIS AND CHARACTERIZATION OF A NOVEL AMPHIPHILIC CORE-CORONA HYPERBRANCHED POLYMER, COMPOSED OF EHMO AND $EHMO_{PEG}$, FOR DRUG DELIVERY

By Khushboo Sharma, M.S.

A thesis submitted in partial fulfillment of the requirements for the degree of Master of Science in Biomedical Engineering at Virginia Commonwealth University.

Virginia Commonwealth University, 2010

Research Director: Dr. Hu Yang
Assistant Professor, Biomedical Engineering

A novel amphiphilic core-corona hyperbranched polymer, composed of 3-ethyl-3-(hydroxylmethyl) oxetane (EHMO) and PEGylated EHMO ($EHMO_{PEG}$), was synthesized through cationic ring opening polymerization. Nuclear Magnetic Resonance spectroscopy (NMR), Dynamic Light Scattering (DLS), and Fourier Transform Infrared spectroscopy (FTIR) were used to characterize the polymer structure and degree of branching. It was found that the degree of branching (DOB) of the polymer was affected by the weight % ratios of $EHMO/EHMO_{PEG}$ used in polymerization. As the weight % ratio of EHMO/ $EHMO_{PEG}$ decreased, the DOB was observed to increase. Polymeric particles based on the synthesized polymer were prepared using the O/W (Oil in Water) solvent emulsion method and evaluated for

drug delivery. Scanning Electron Microscopy (SEM) and Dynamic Light Scattering (DLS) were used to characterize the size and shape of the particles. The obtained particles were found to be spherical in shape and have a narrow size distribution. Camptothecin (CPT) was used as the model drug for drug encapsulation and controlled release studies. The loading and encapsulation efficiencies of the particles ranged between 60% and 80%. Cytotoxicity studies carried out with human skin fibroblasts indicated that as the weight % ratio of the EHMO/ $EHMO_{PEG}$ decreased the biocompatibility of the polymer increased. In vitro drug release studies showed that the CPT could be released over an extended period of time. The efficacy of the drug released from the particles was demonstrated by the MTT assay on HN12 cells. The results showed that the cellular activity decreased as the amount of drug released from the particles increased over a span of 72 hours. The synthesized polymer represents a new family of hyperbranched macromolecule with potential for drug delivery.

CHAPTER 1 INTRODUCTION

For a long time, pharmaceutical formulations mostly comprised quick acting and simple substances that could be easily administered either orally or injected directly.[1] However, over the last few decades, the scenario has been changing and the need for formulations with controlled release and specificity has increased significantly.[1] Various efforts are being centered on not only the synthesis of better vehicles to carry drug formulations but also their administration routes. The encapsulation of drugs into a delivery vehicle for site specific delivery has become an important strategy to reduce degradation of drugs, which otherwise reduces and limits their efficacy before they reach a specified site for action.[2] Additionally, these vehicles are designed to overcome various problems such as drug toxicity, burst release, etc.[1, 2] A number of drug delivery systems have been developed for drug delivery, including liposomes, microspheres, and nanoparticles.[3, 4] Polymeric drug delivery systems are attractive vehicles for drug delivery as they can serve as a means of effectively controlling drug dose and for targeting specific regions in the body.[1] The use of polymeric drug delivery systems for example poly(lactic acid) based delivery system, dated back to early 1970s.[1] Most polymers being investigated for drug-delivery applications are either linear (non-branched) or cross-linked in nature.[5-7] Recent developments in polymers with hyper branched and defined architectures have opened new opportunities for developing more efficient drug delivery systems.

This thesis work involves synthesis and characterization of a novel amphiphilic core corona hyperbranched polymeric system. This polymeric system was explored as a carrier for delivery of hydrophobic drugs. Cationic ring opening polymerization was used for the synthesis using 3-ethyl-3-(hydroxymethy) oxetane (EHMO) and PEGylated EHMO ($EHMO_{PEG}$) as monomers. Four different polymers were prepared by varying the molar ratios of EHMO/ $EHMO_{PEG}$ for this study. Techniques such as Fourier Transform Infrared spectroscopy, Scanning Electron Microscopy, Dynamic Light Scattering, Differential Scanning Calorimetry and Nuclear Magnetic Resonance spectroscopy were used to characterize the synthesized monomer and polymers. This hyperbranched polymer was further formulated into particles using single oil-in-water (O/W) emulsion/solvent method and evaluated for delivery of anticancer drug camptothecin.

CHAPTER 2 BACKGROUND

2.1 A brief history of branched polymers

Vogtle was the first to introduce the idea of hyperbranched polymer.[8] This study led to the concept of insistent growth, which was applied to the synthesis of low molecular weight amines.[8] Before this discovery, there were only three major polymer classes based on polymer architecture – linear, crosslinked and branched.[5-8] After the iterative reaction scheme was identified, many researchers have developed interests in exploring synthesis and applications of such hyperbranched structures. Macromolecular architectures of branched polymers can be divided into three major classes: dendrimers[3], dendrigrafts[3], and hyperbranched polymers.[5] Since then a number of hyperbranched polymers including dendrimers have been developed, such as poly(propylene imine) (PPI) dendrimers by Wörner/ Mülhaupt[9] and Brabender-van den Berg/Meijer[10], poly(amidoamine) (PAMAM) dendrimers by Tomalia et al.[11, 12] and dendri-poly(ethers) along with dendripoly(thioethers) by Newkome et al.[13, 14]

2.2 Dendrimers

Dendrimers are the best characterized subclass. They possess unique properties such as mono-dispersity and highly symmetrical structure. Their basic architectural components include a core, interior units comprising of various branches and surface functional groups.[7, 8, 15] Dendrimers are formed by repetitive sequence of reaction steps, where with

each successive step molecular weight and generation number become higher than the previous[7]. Two common ways applied for dendrimer synthesis are convergent and divergent methods. The divergent method as shown in Figure 1,[15, 16] involves the addition of monomer and then the subsequent building up of the structure from the core eventually proceeding outwards to the periphery of the molecule.[7, 8, 15] The symmetric branched structure is formed by covalently attaching a new generation to the reactive sites present in the core.[7, 15] In this method the number of reactions increase exponentially for each subsequent generation.[7, 15] Reaction at each step of synthesis must be completed in order to avoid any trailing generation that might form if some branches are shorter than the others. These impurities might impair the functionality and symmetry of the dendrimer.[7, 15]

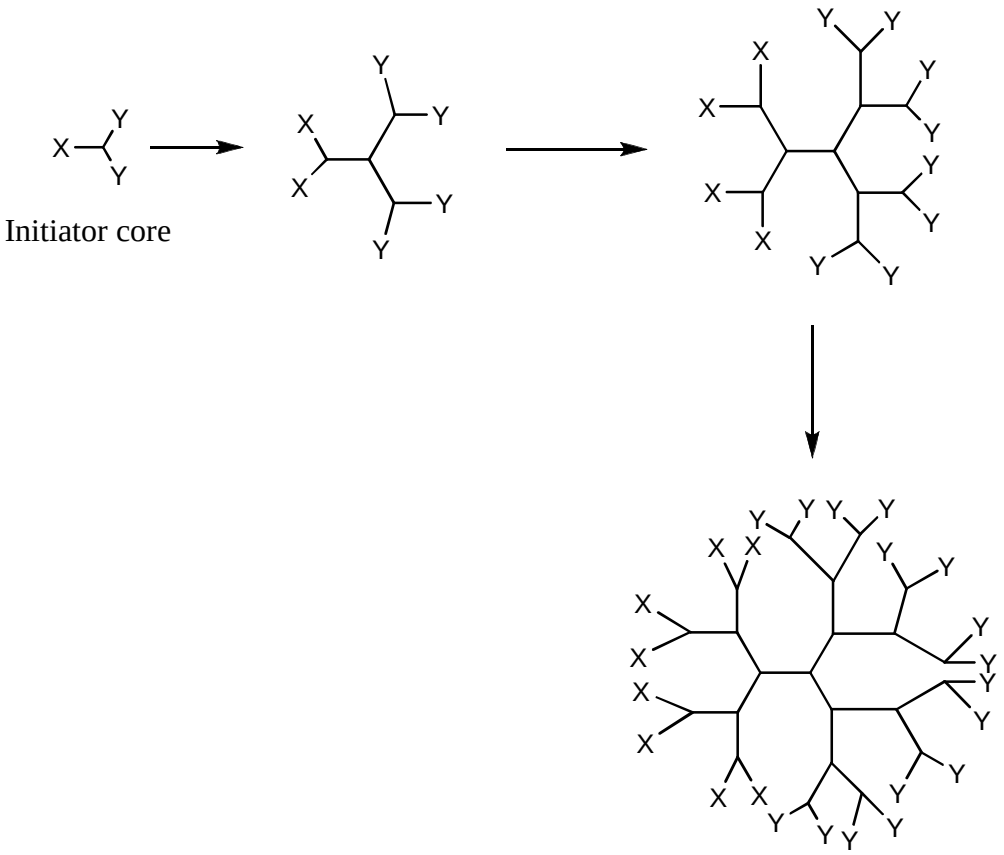

Figure 1: Divergent method of dendrimer synthesis.

The convergent method as shown in Figure 2, [15, 16]uses small terminal moieties or groups attached to a monomer with masked functional groups for initiating the process.[7, 15] In this method, the reaction and growth proceed from outside to inward towards the core.[7, 15] This method has advantages including easy removal of impurities to help sustain the functionality of dendrimer, and reduction of the number of transformations required to connect every consecutive generation.[7, 15] However, sterical hindrances cause crowding and hence the generation of dendrimers formed by this method is not very high.[7, 15]

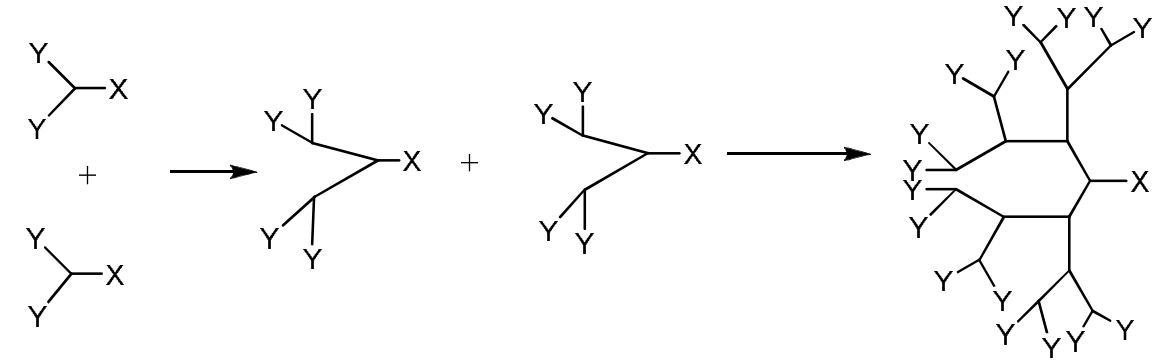

Figure 2: Convergent method of dendrimer synthesis.

Some examples of the polymers prepared by the divergent method are poly(amidoamine) (PAMAM)[11, 12] and poly(propylene imine) (PPI) dendrimers[11, 12] and those prepared by the convergent method are poly(benzyl ether) dendrimers.[11, 12] Their molecular weights can be controlled as required.[7, 17] The number of their surface functional groups increases exponentially while their diameter increases linearly with increase in generation.[5] Their surface functional groups play a significant role in determining material properties and can be modified to get a desired property.[5, 18] Dendrimers, have lower viscosities and higher solubility than their linear analogues.[5, 19]

2.3 Dendrigraft polymers

Another subset of hyperbranched polymers are dendrigraft polymers,[20, 21] which are known as semi-controlled polymers as their structures are not as well defined as dendrimers.[3] Similar to dendrimers, dendrigraft polymers consist of a core, interior with branches and various terminal functional groups. However, unlike dendrimers, their grafting sites are

distributed quite randomly.[3] They can be prepared by divergent 'grafting onto' method as shown in Figure 3.[21] Some examples of successfully synthesized dendrigrafts are poly (2-ethyl-2-oxazoline) (PEOX) oligomers grafted onto linear poly(ethylene imine) substrates.[20]

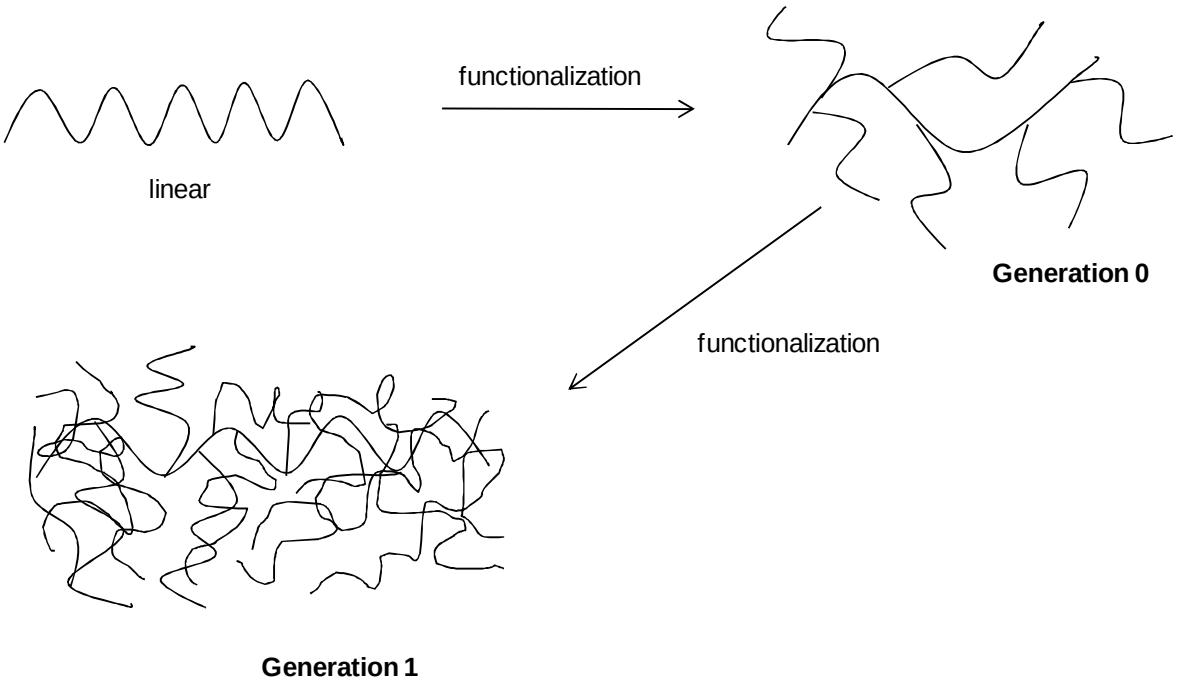

Figure 3: Synthesis of dendrigraft polymer.

2.4 Hyperbranched polymers

Hyperbranched polymers have received considerable attention in recent years due to their versatile architecture and many potential applications.[3, 22] They have been exploited as drug delivery vehicles because their architecture can be aptly modulated to obtain desired properties. For instance, functional groups on the surface can be engineered to influence their properties such as glass transition temperature, solubility, mechanical properties, and melt viscosity.[22, 23] Hyperbranched polymers are poly-disperse but less complicated to

synthesize when compared to dendrimers.[22, 24, 25] Their cost-effective manufacturing makes them attractive for large scale applications. One of the most attractive features of hyperbranched polymers is the absence of entanglement and low viscosity in bulk and solution.[5] Different methods including self poly-condensation polymerization, proton transfer polymerization, and ring opening chain polymerization have been exploited for the synthesis of hyperbranched polymers.[22, 24]

2.4.1 Methods for synthesis of hyperbranched polymers

There are two major methods used for the polymerization of hyperbranched polymers: single monomer methods (SMM),[26] where only monomer AB_x is required for polymerization; and double monomer methods (DMM),[26] where the polymerization requires two different types of monomers.

2.4.1.1 Polycondensation of AB_x monomers

Self poly-condensation is a one step reaction, which is useful for polymerization of AB_x monomers.[27-29] Examples of polymers prepared by this method are polyethers,[27-29] polyesters,[30] and polycarbonates.[31] The reaction is shown in the following scheme (Figure 4).[22]

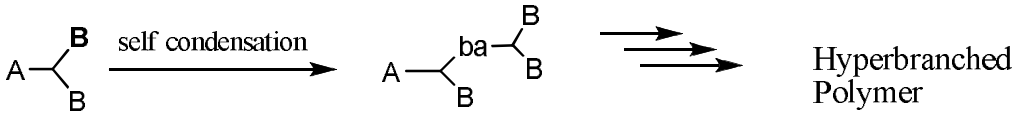

Figure 4: Self poly-condensation of AB_2 monomer

Requirements for self poly-condensation vinyl polymerization (SCVP) are a double bond and an initiation moiety in the monomer. The reaction takes place in the following manner (Figure 5).[22]

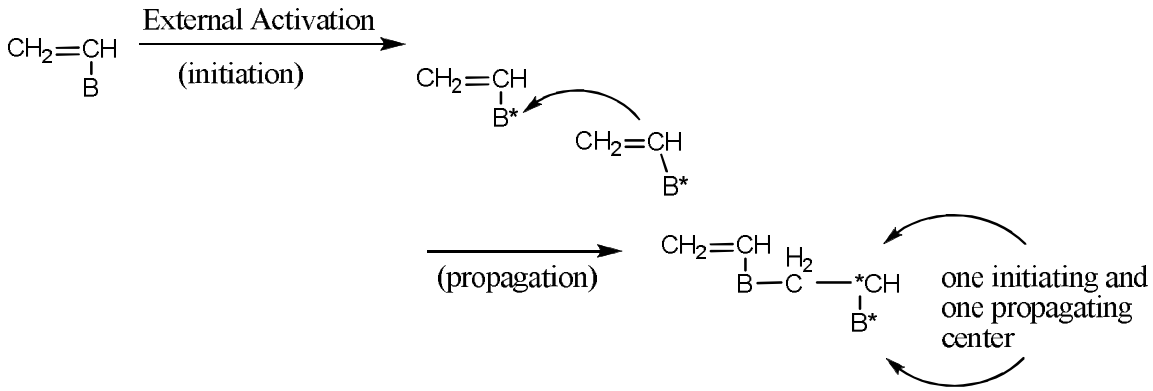

Figure 5: Self poly-condensation vinyl polymerization

2.4.1.2 Proton-transfer polymerization (PTP)

PTP is dependent on the basicity and acidity of monomers as shown in Figure 6.[32] This concept has been used for synthesis of various hyperbranched polymers such as an aliphatic hyperbranched polyether derived from a diepoxide and a trifunctional alcohol group.[33, 34]

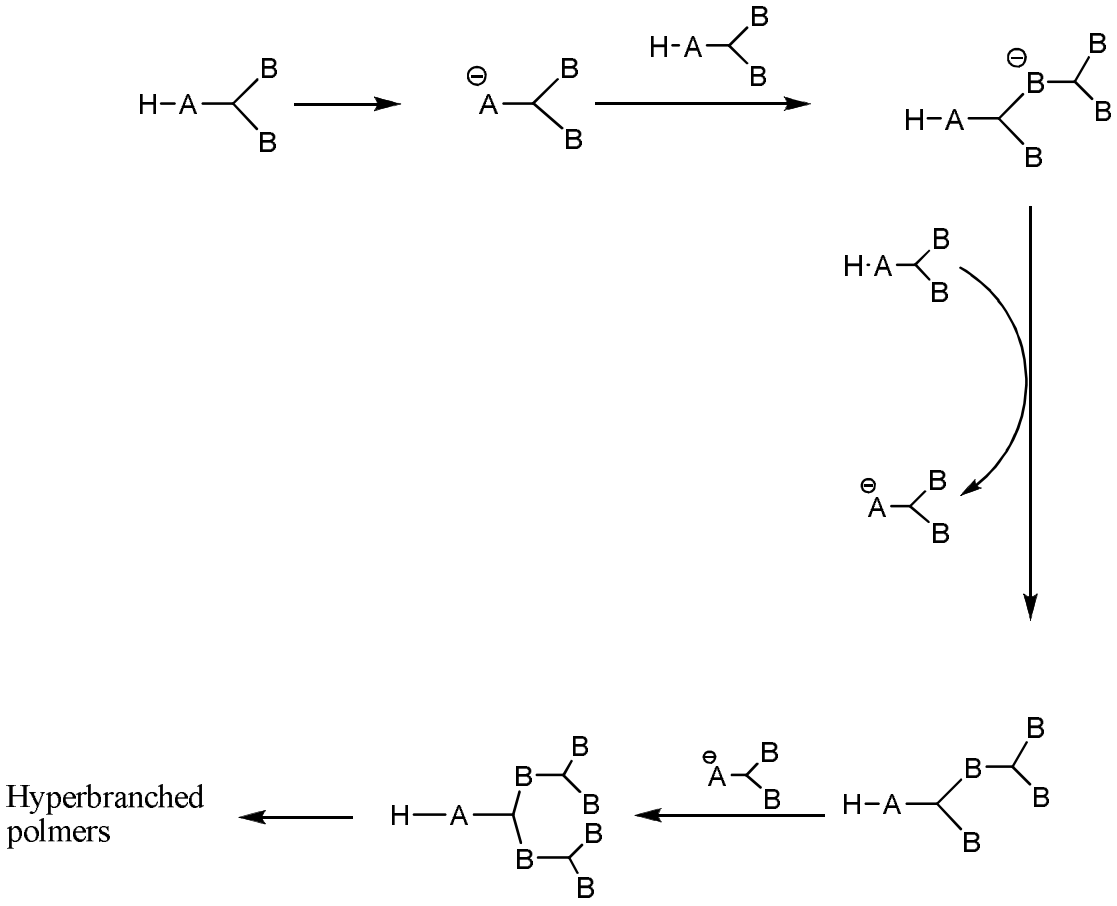

Figure 6: Proton transfer polymerization.

2.4.1.3 Ring-opening polymerization (ROP)

The third method is the ring opening polymerization which was earlier known as multi-branching polymerization since the number of chain terminals increases with progression of polymerization.[7, 24] Molecular weight distribution of the polymers generated by this method can be controlled by moderating the addition of proper initiators to generate various numbers of active sites.[7, 24] One of the examples of ring opening polymerization is shown in Figure 7.[22]

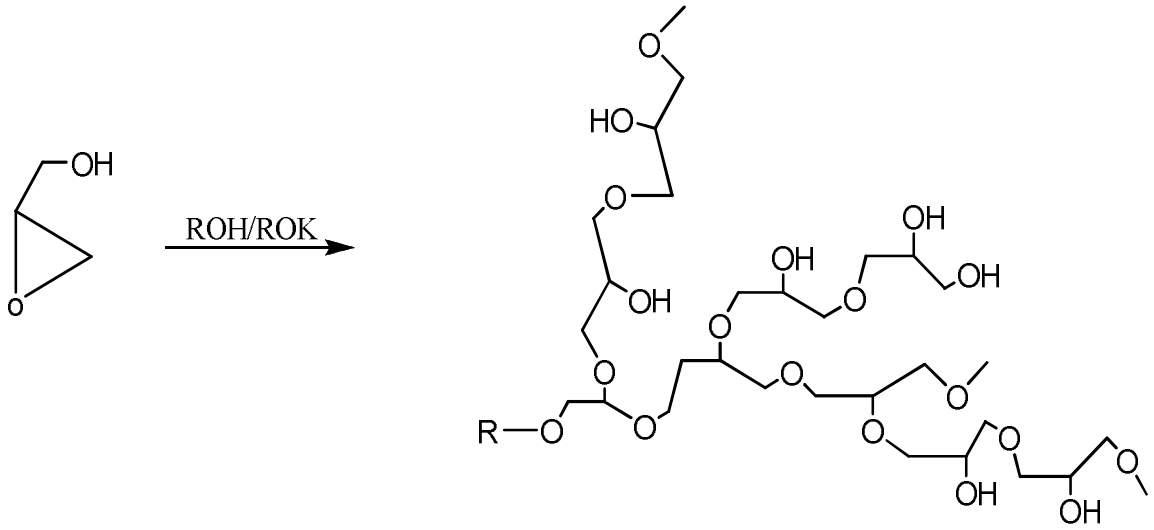

Figure 7: Ring opening polymerization.

2.4.2 Degree of Branching

For maximizing the advantages of hyperbranched polymer, it is important to understand their structure-property relationship.[6, 35] Degree of branching is one of the most important aspects of this relationship. Hyperbranched polymers consist of dendritic unit (D), linear unit (L), and terminal unit (T) as shown in Figure 8,[22] which influence the degree of branching of the polymer.[6, 35]

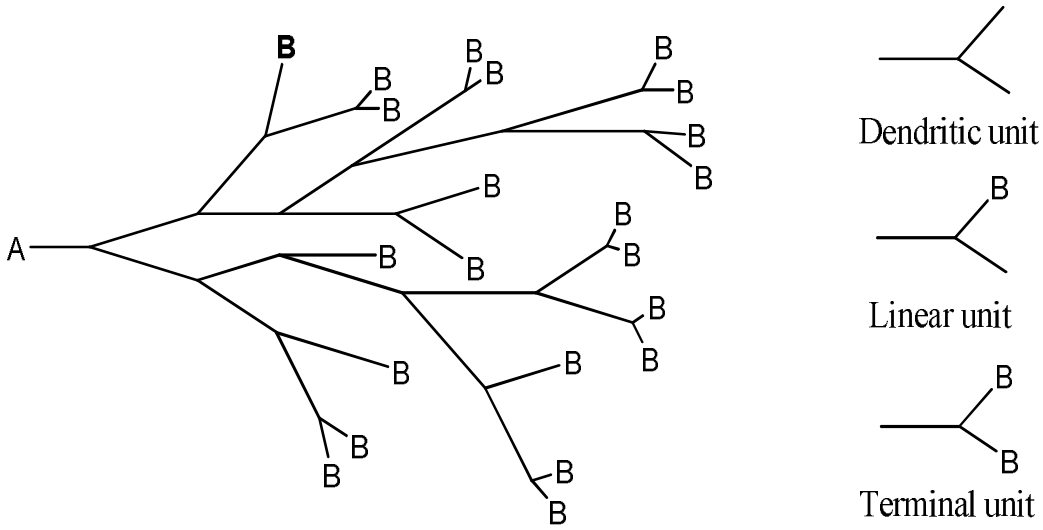

Figure 8: Degree of branching.

Degree of branching can be calculated by the following equation.[6, 23]

$$DOB = \frac{D+T}{D+L+T}$$

Values for dendritic units, linear units, and terminal units can be determined by integrating the corresponding peaks in ^{13}C NMR. Degree of branching has a huge impact on hyperbranched polymer's physical and chemical properties. Recently it was reported that the degree of branching could be controlled by many factors including monomer to catalyst ratio, and temperature. It has been proposed that the degree of branching increases with temperature.[36]

2.4.3 Properties of hyperbranched polymers

Glass transition temperature governs the thermal behavior of hyperbranched polymers.[37] Factors such as chain end groups, molar mass and macromolecular composition influence the glass transition temperature of a given polymer.[37] Increase in the degree of branching results in a change of the glass transition temperature, which can be explained using free volume concept.[38] Particularly, polymers with more branches occupy more free space. Therefore, the restriction in the movement of the chains can only be overcome at higher temperature.[5, 22, 24] Due to less entanglements and more organized branched structure, hyperbranched polymers have different mechanical properties from crosslinked polymers[5, 22, 24] Because of their globular structure, chain extension and orientation become difficult, hence resulting in strain hardening. Melt viscosity of hyperbranched polymers is much lower than that of their linear polymers.[20, 21] Intrinsic viscosity (as described by the Mark-Houwink equation) and hydrodynamic volumes are lower for hyperbranched polymers than for their linear analogues due to differences in their structural arrangement.[5]

2.5 Drug delivery

Drug delivery systems can help improve the specificity, bio-distribution and efficacy of drugs.[1, 2] Since polymers have a capacity of being customized, they are good substitutes to replace the earlier established carriers such as viruses, and protein conjugates which have limitations such as poor stability and non-specificity.[1, 2] Several commonly used methods for drug delivery based on polymers are polymer-drug conjugate,[1, 2] drug encapsulating polymeric micelles,[1, 2] and multicomponent polyplexes.[1, 2] Encapsulation of a drug in the

polymeric micelles is realized by trapping the drug in the internal core through hydrophobic-hydrophobic interactions. Polymer-drug conjugates, on the other hand, are usually prepared by covalently coupling drug to polymer.[1, 5] Polymeric nanoparticles have shown great promise as drug carriers in the biomedical field.[4, 39] Nanoparticles can be one of two types: firstly monolithic nanocapsules[1, 2, 39] in which drug is encapsulated in the hydrophobic or hydrophilic core surrounded by a shell; and secondly nanospheres[1, 2, 39] which can encapsulate the drug through out the entire matrix.[1, 2] They help overcome hurdles that are usually faced with direct administration of drugs. They increase the solubility and action specificity of drugs.[2,23,39] They are small in size and easy to administer and result in high cellular uptake. [2, 39] The most important property they possess is their ability to release the entrapped drug in a well controlled manner.[1, 23] Amphiphilic polymers play an important role in the delivery of hydrophobic drugs.[23, 39] They arrange themselves in a manner where the hydrophobic drug can be encapsulated in the polymer's hydrophobic. Meanwhile, a hydrophilic PEG layer offers stealth properties to the vehicle and help extend its half life.[1, 2, 23]

3-ethy-3-(hydroxymethyl) oxetane was selected as the monomer **1** for polymerization as it is a trifunctional monomer which can be reacted to form a hyperbranched structure. Monomer **2** was synthesized by attaching a PEG chain to monomer **1** to provide biocompatibility to the monomer, which could further be imbibed in the polymer.

CHAPTER 3 MATERIALS AND METHODS

3.1 Materials

Table 1: List of materials used

Material	Abbreviation
3-ethyl 3-(hydroxymethyl) oxetane (monomer **1**)	EHMO
Boron trifluoride diethyl etherate	
Dichloromethane	DCM
Chloroform	
Methanol	
De-ionized water	DI water
Triethyl anhydride	TEA
4-nitro phenyl chloroformate	NPC
Tetrahydrofuran	THF
Dimethylformamide	DMF
Dimethyl Sulfoxide	DMSO
Hexane	

3.2 Equipment

Table 2: List of equipments and machines used:

Equipment name	Use
Nuclear Magnetic Resonance (NMR)	400 MHz spectrometer was used to carry out proton and carbon13 measurements
Dynamic Light Scattering (DLS)	To measure the hydrodynamic radius of nanoparticles and also to measure molecular weight of the polymers
Flexi-dry MP controlled rate freezer (FTS systems, Inc.)	To freeze dry the samples
Differential Scanning Calorimetry (DSC)	To determine the glass transition temperature of the polymers
Scanning Electron Microscopy Model EVO 550	To take photographs of the nano-particles
UV-Vis spectrophotometer	To conduct quantitative analysis for drug release studies
Eppendorf Centrifuge Model- F-45-24-11	To centrifuge samples to separate liquid phase from suspended phase
Fourier Transform Infrared spectroscopy (FT-IR)	For characterization of the polymer

3.3 Synthesis

3.3.1 Monomer synthesis

PEGylated EHMO (i.e., monomer **2**) was synthesized by substituting the hydroxyl group present on 3-ethyl 3-(hydroxymethyl) oxetane with NH_2-PEG-OCH_3 (MW= 2000 daltons and 550 daltons) group as described in a previously reported method.[23]

Method of preparation of monomer **2**:

As shown in Scheme 1, monomer **1** (0.29 g) was weighed and dissolved in 5 ml of THF. To this solution, 0.252 g (347 µl) and 0.500 g NPC were added. The mixture was stirred for 24 hours and then centrifuged at 5000 rpm for 20 minutes to remove the salt. The supernatant was collected and rotovaporated to remove the solvent. The obtained dry product was further reacted with NH_2-PEG-OCH_3 (0.335 gm) in 5 ml of DMF at room temperature. After 72 hours, dialysis was performed for the purification of the final product using a 500 molecular weight cut off membrane (500 MWCO). The sample obtained after dialysis was freeze dried to get dry monomer **2** ($EHMO_{PEG}$) with a yield of 60%.

Calculation:

Weight of the intermediate product obtained = 281 g/ mole

Amount of intermediate product being used = 0.05 g which is equivalent to $1.77*10^{-4}$ moles

Molecular weight of NH2-PEG-OCH3 being used = 2000 g/ mole

Since we want to keep the molar ratio as 1:1 therefore amount of PEG to be used = 0.335 g ($1.77*10^{-4}$ moles)

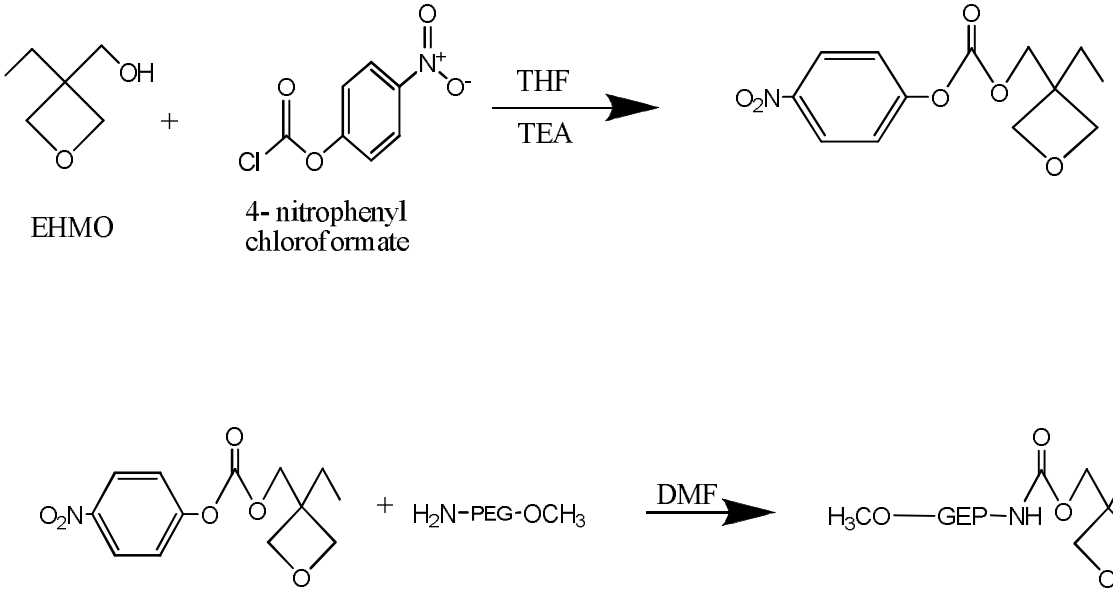

Scheme 1: PEGylated monomer synthesis

3.3.2 Synthesis of polymer

Cationic ring opening polymerization[40, 41] was used for synthesis of hyperbranched polymer as shown in Scheme 2. The reaction was carried out in a three necked round bottom flask using a PTFE stirrer for mixing. The glassware used was washed well and dried in oven for few hours. The whole reaction set up was first degassed and dried completely by passing nitrogen from it for 30 minutes. The flask was placed on a heating mantle with temperature maintained at 100°C for first half an hour and then at 45°C for rest of the reaction. At 30 minutes, the nitrogen source was removed and the solvent,

dichloromethane (15 ml) and the catalyst $BF_3O(C_2H_5)_2$ were added to the flask. Within five minutes the monomer **1** was introduced and the flask temperature was maintained constant at 45°C. After the reaction was allowed for 48 hours, monomer **2** was added in to the flask and the reaction proceeded for another 24 hours. At the end of 72 hours the reaction was quenched by ethanol. The resultant polymer was dried in the vacuum oven at 60°C for two days. Four different poly(EHMO-$EHMO_{PEG}$) co-polymers with various monomer **1**: monomer **2** ratios (i.e.98.2:1.8 wt%, 96:4 wt%, 74.4:25.6 wt%, 17:83 wt%) were prepared. The first three polymers were prepared using EHMO modified with PEG chain of 2000 daltons and the last polymer with ratio 17:83 wt% (EHMO/$EHMO_{PEG}$) was prepared using the monomer with a shorter PEG chain (MW= 550 daltons). This was done in order to reduce the steric hindrance in the polymerization and also to determine its influence on properties of the polymers. The yields of the obtained polymers ranged between 50-66% being highest for 98.2:1.8 and lowest for 17:83 polymeric ratios. The synthesized polymers are reproducible.

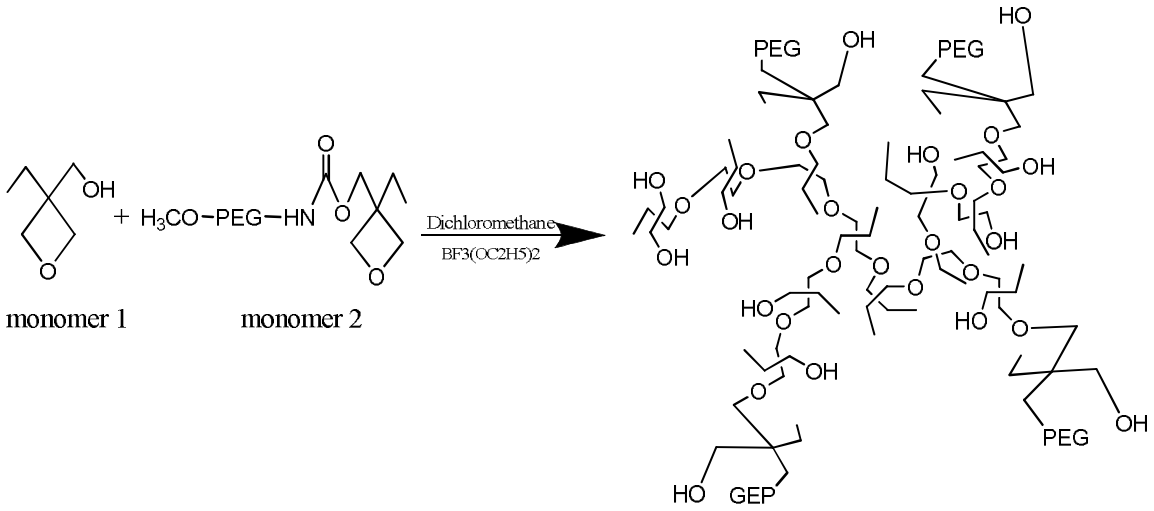

Scheme 2: Polymer synthesis

3.3.3 Preparation of polymeric particles

Single oil-in-water (O/W) emulsion/ solvent evaporation method[23, 42] was used to obtain blank and drug loaded nanoparticles. The synthesized polymers (10 mg) were dissolved in 1 ml of chloroform and 2 ml of DI water was drop wise added under magnetic stirring to prepare the blank particles.[23]

Camptothecin, a hydrophobic anti cancer drug,[43, 44] was used as the model drug. Drug solution was prepared by dissolving 10 mg of drug in a mixture of chloroform: methanol (4:1). Drug loaded nanoparticles were prepared by adding the drug solution (10 mg/ml) to the polymer solution (10 mg/3 ml). The mixture was kept at room temperature overnight. The equilibrated solution was then rotovaporated to remove the solvents. The particles

subjected to centrifugation for 1 hour at 13,200 rpm were collected and dried completely under vacuum.

3.4 Characterization

3.4.1 Nuclear magnetic resonance spectroscopy

^{1}H and ^{13}C NMR spectra were taken to confirm the synthesis of the monomer and the polymer on a 400 MHz Bruker NMR instrument. Chloroform-d6, DMSO- d6, D_2O were used as solvents and tetramethylsilane (TMS) was used as an internal standard. Processing of the data obtained was performed using "spin works" (free software) software courtesy of the University of Manitoba, Canada. The chemical shifts for the respective solvents are as follows:

Table 3: NMR shifts for commonly used solvents

NMR spectroscopy solvent		Chemical shift (ppm)
Carbon shifts	D_2O	
	DMSO- d6	40.4
	Chloroform- d6	77.3
Proton shifts	D_2O	4.8
	DMSO- d6	2.5
	Chloroform- d6	7.2

Degree of branching was also calculated using 13C-NMR. The triplet peaks obtained at 43 ppm were integrated to obtain the values. Integration of the first peak, second peak and the third peak provided the values for the dendritic(D) units, Linear(L) unit, and the terminal(T) units as shown in Figure 8.

3.4.2 Differential scanning calorimetry

DSC Q-1000 (TA instrument) was used for thermal analysis by determining glass transition temperature (T_g) and melting temperatures (T_m) of the synthesized polymers. Samples were prepared by placing 5-6 mg of polymers in hermetic pans with lids. In the process, the samples were first equilibrated at -40°C and then ramped up to 100°C using a heating rate of 10°C per minute and then cycle 2 was run at a cooling rate of 10°C per minute. The data included is after cycle 2.

3.4.3 Fourier transform infrared spectroscopy

FT-IR was also run on a Nicolet magna IR 760 spectrometer to identify and determine the different groups present in the polymer synthesized. Plots of % transmission and wavelength were plotted. Samples were prepared by placing 1-2 mg of polymer on the KBr (potassium bromide) disc and drying it with a drier.

3.4.4 Dynamic light scattering

Zetasizer Nano ZS Instrument from Malvern Instruments was used to determine the size of the particles and molecular weight of the polymer.[45, 46] Dynamic light scattering is a noninvasive method which works on the principle of light scattering and determines the molecular weight and size of the particles by enforcing the Rayleigh equation.[45, 46] Laser is used as the light source. When the light falls on the particles, scattering of light takes place and molecular weight is determined by the measurement of the time averaged intensity of scattered particles. The working principle of the process is as shown in the Figure 9.[47]

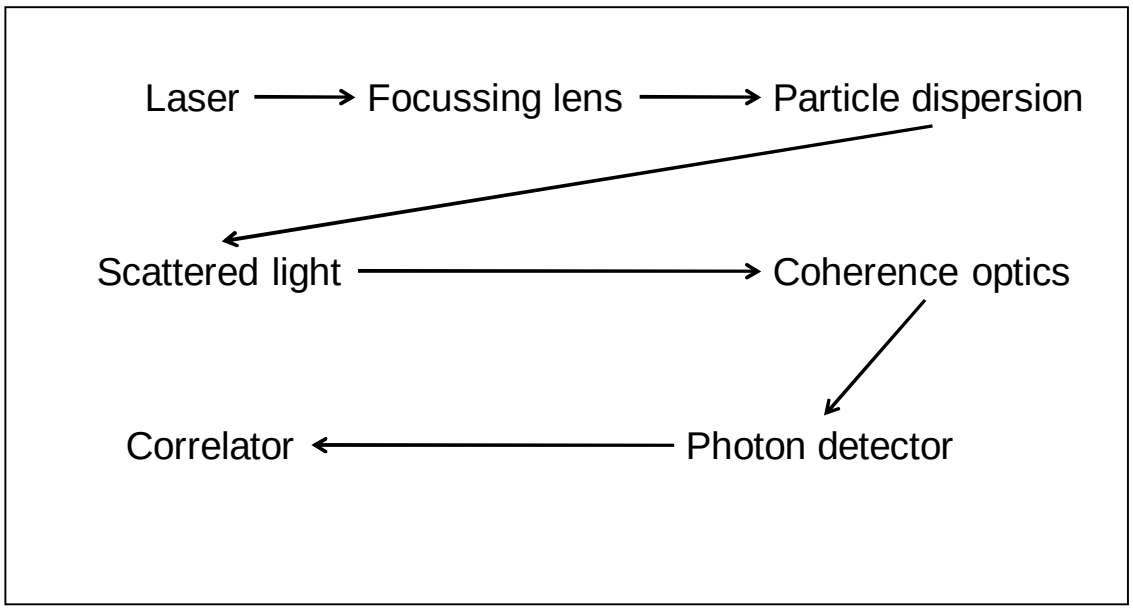

Figure 9: Working principle of DLS

Intensity of the scattered light is proportional to the product of the weight average molecular weight and the concentration of the solution. Debye plot between intensity of scattered light and concentration is used for the calculation. The intercept yields the inverse of the weight average molecular weight and toluene is used as the standard due to its high Rayleigh ratio which helps in accurate measurement. [45, 48]

Rayleigh equation:

$$KC/R = (1/M + 2A2C) P$$

From Debye plot:

KC/R is proportional to 1/ (molecular weight in Daltons)

The size of the particles was obtained on the basis of the same principle. Samples for blank nanoparticle size measurement studies were prepared by dissolving 1 mg of polymer in 1ml of chloroform and then adding 2 ml water under magnetic stirring at room temperature.

3.4.5 Scanning electron microscopy

SEM was performed at the department of Anatomy and Neurobiology, (facility funded by NIH-NINDS Center core grant 5P30NS047463 and NIH-NCRR grant 1S10RR022495) to observe the morphology of the blank and drug loaded nanoparticles and also estimate their diameter. Zeiss EVO-50XVP model was used with an accelerating voltage of 10kV. Samples were prepared by putting few drops of the nanoparticle solution on a small cut silicon wafer and drying it for 6 hours in vacuum. Each sample was gold sputter coated (EMS 550 Automated sputter coater, Electron Microscopy Sciences) prior to its use. The images were taken at 35000x magnification. The working principle of the scanning electron microscopy is as shown in Figure 10.[49]

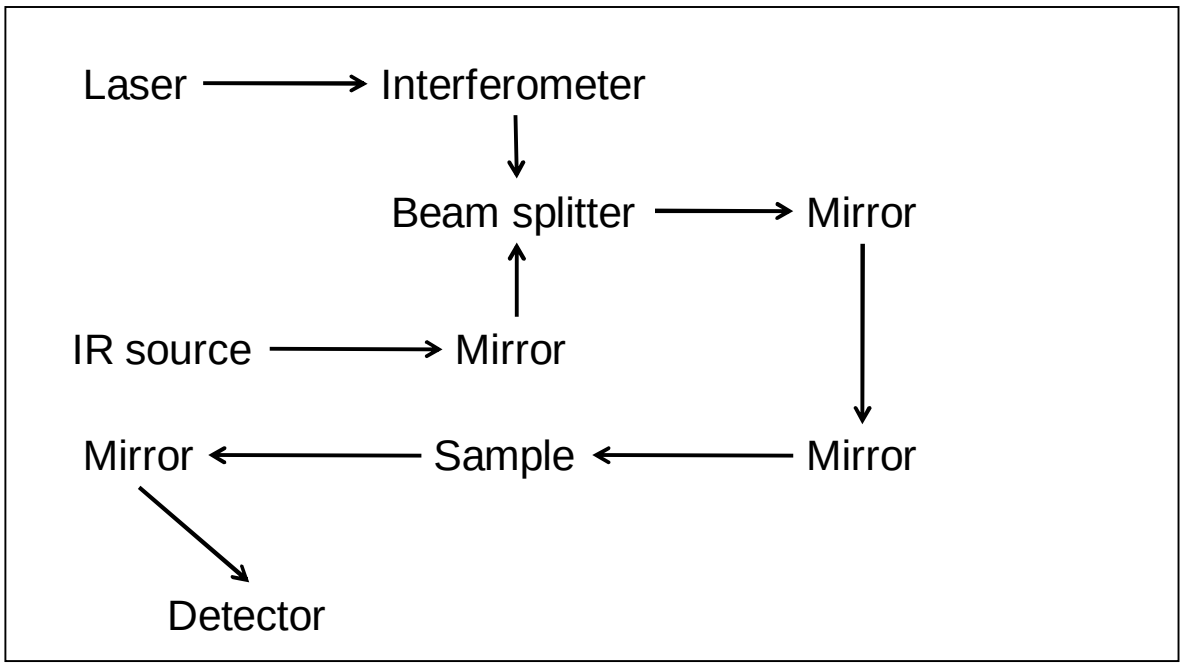

Figure 10: Working principle of SEM

3.5 Drug loading and encapsulation efficiency studies

Camptothecin, an anticancer hydrophobic drug, was used as a model drug[43, 44] Before conducting any drug release studies, a scanning curve for CPT (Figure 11) was taken out using 1mg/ml solution of CPT in a mixture of chloroform and methanol (4:1) and since the absorbance values were highest at a wavelength of 369 nm, it was used to plot the standard curve (Figure 12) using UV-visible spectrophotometer. UV-visible spectroscopy was used to determine the amount of CPT that was encapsulated by the nanoparticles prepared.[23] The drug loaded nanoparticles were weighed and divided in to three equal amounts. Then all three samples were dissolved in a mixture of chloroform and methanol solvents (in the ratio of 4:1). The samples were centrifuged for one hour at a speed of 13,200 rpm. After one hour the absorbance values were measured at 369 nm. The drug encapsulation

efficiency (EE) is defined as the percentage of the drug in the nanoparticle with respect to the total amount of drug used and the loading efficiency (LE) is measured as the amount of drug encapsulated in the nanoparticle with respect to the total amount of the nanoparticles as shown in the following equations.[23, 50]

EE = (Total amount of CPT- Free amount of CPT) / Total amount of CPT

LE= (Total amount of CPT- Free amount of CPT) / Total amount of nanoparticle

3.6 Cytotoxicity studies

To evaluate the cytotoxicity of the synthesized polymeric particles, human dermal fibroblasts (obtained from Dr. Gary L. Bowlin's lab, Biomedical Engineering department, VCU) cultured in Dulbecco's modified Eagle's medium (DMEM) supplemented with 10% fetal bovine serum (FBS) were used. The fibroblasts cells were incubated with blank polymeric particles at different concentrations (0.01µg/µl, 0.05µg/µl, 0.1µg/µl, and 0.33µg/µl) at 37 °C for 48 hours. The cell viability was assessed with the MTT assay. Another cellular assay (MTT test) was performed to determine the efficacy of the drug loaded particles on the HN12 cells (derived from metastatic Squamous Cell Carcinoma). In this study, poly(EHMO-$EHMO_{PEG}$)$_{50:1}$ with a final concentration of 0.01µg/µl was studied

3.7 Drug release study

Drug loaded polymeric particles were weighed and dissolved in 10 ml of PBS buffer in a capped conical flask. The solution was maintained at 37 °C. At predetermined intervals

the entire solution was centrifuged at 3500 rpm for 15 minutes. Afterwards, 3 ml of supernatant was collected and subjected to UV-visible measurement at 369 nm to quantify the released drug. After each measurement, 3 ml of fresh PBS buffer was added back to medium.[23]The drug release was calculated in terms of cumulative release by keeping in to account the amount withdrawn at every measurement point. The concentration of drug at each time point was calculated using the standard curve (Figure 12).

Calculation:

$$\text{Relative amount released } (t_0) = \frac{[\text{concentrartion}]_{t0} * 10\ \text{ml}}{10\ \text{mg loading drug}}$$

$$\text{Cumulative amount released (t)} = \frac{([\text{concentration}]_t * 10\ \text{ml} + [\text{concentration}]_{t0} * 3\text{ml})}{10\ \text{mg loading drug}}$$

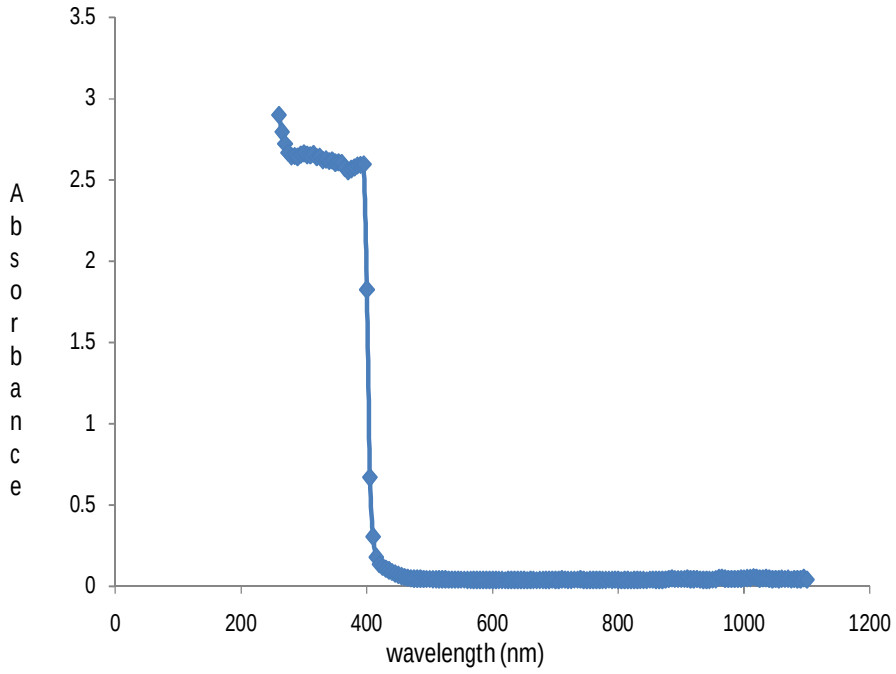

Figure 11: UV-Vis Scan of CPT (1 mg/ ml)

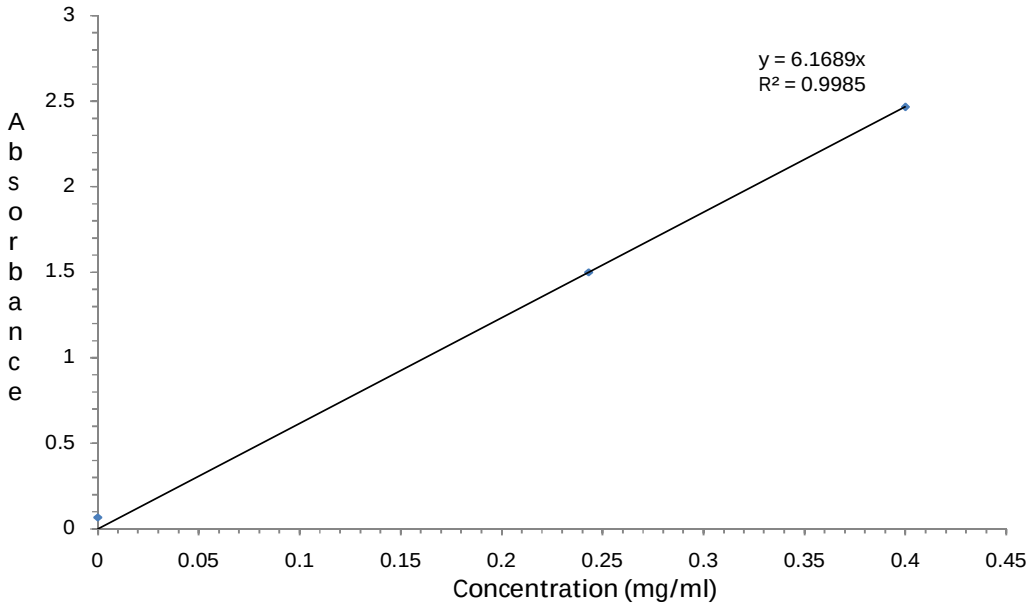

Figure 12: Standard Calibration Curve of CPT (360 nm)

CHAPTER 4 RESULTS AND DISCUSSION

4.1 Preparation and characterization of $EHMO_{PEG}$ and poly(EHMO- $EHMO_{PEG}$)

NMR spectroscopy (400 MHtz) was used to confirm the synthesis of the PEGylated monomer and the poly(EHMO- $EHMO_{PEG}$). In the ^{1}H-NMR of the monomer **1**, EHMO (Figure 13b), the peak at 4.3ppm is distinctive of the protons present in the oxetane ring of the EHMO. ^{1}H-NMR for the monomers (Figure 13) displayed the following peaks which correspond to the respective groups.

Table 4: ^{1}H-NMR shifts for monomer characterization

Chemical shift (ppm)	Group(s)
4.4	-C<u>H</u>$_2$ groups of the oxetane ring
0.9	-C<u>H</u>$_3$ group on the oxetane side chain
1.7	-C<u>H</u>$_2$ group on the oxetane side chain
3.7	-CH$_2$-O<u>H</u>

According to ^{1}H-NMR spectrum of the polymer (Figure 14 B), disappearance of the peak at 4.3ppm indicates the occurrence of the ring opening polymerization.

The following other peaks were also observed:

Table 5: ^{1}H-NMR for polymer characterization

Chemical shifts (ppm)	Group(s)
0.9	-C<u>H</u>$_3$ groups
1.7	-C<u>H</u>$_2$ groups
3.1	-C<u>H</u>$_2$-O group
3.3	-C<u>H</u>$_2$-OH
3.8	-O<u>H</u> group
3.5	-(C<u>H</u>$_2$C<u>H</u>$_2$) group
3.75	-(OC<u>H</u>$_3$) group
5-8	-(N<u>H</u>) group

Table 6: ^{13}C-NMR for polymer characterization

Chemical shifts (ppm)	Group(s)
9.9	-<u>C</u>H$_3$ groups
21.8	-<u>C</u>H$_2$ groups
43	-D+L+T groups
72	-(<u>C</u>H$_2$<u>C</u>H$_2$) groups
62	-<u>C</u>H$_2$OH group

Figure 13: ^{1}H-NMR spectra of monomers

a) $EHMO_{PEG}$

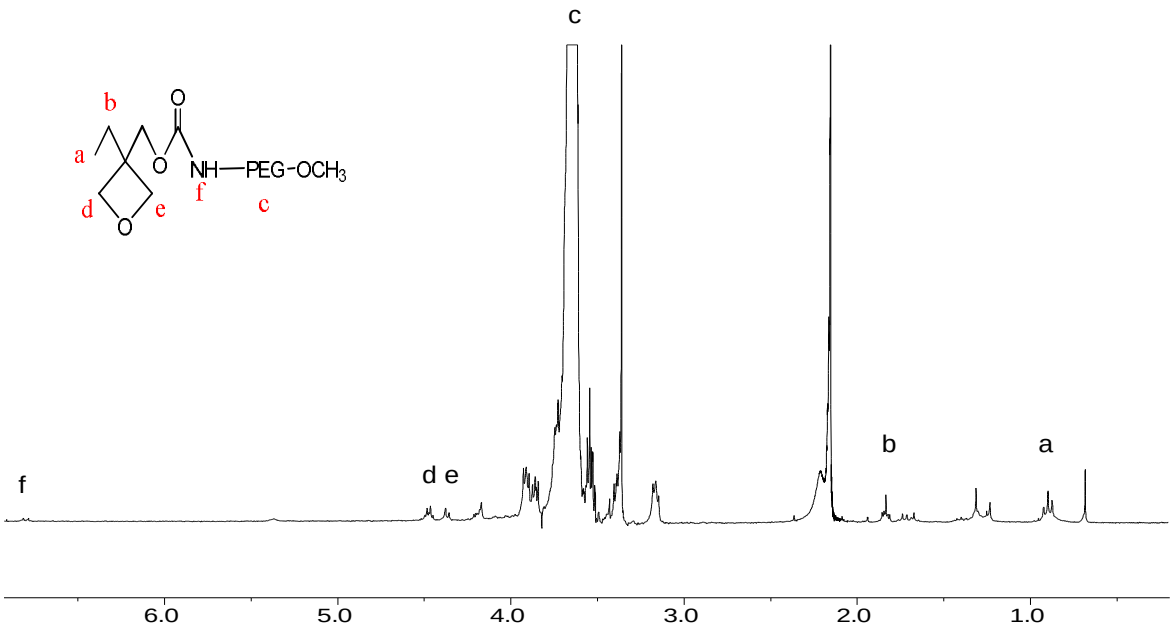

b) EHMO

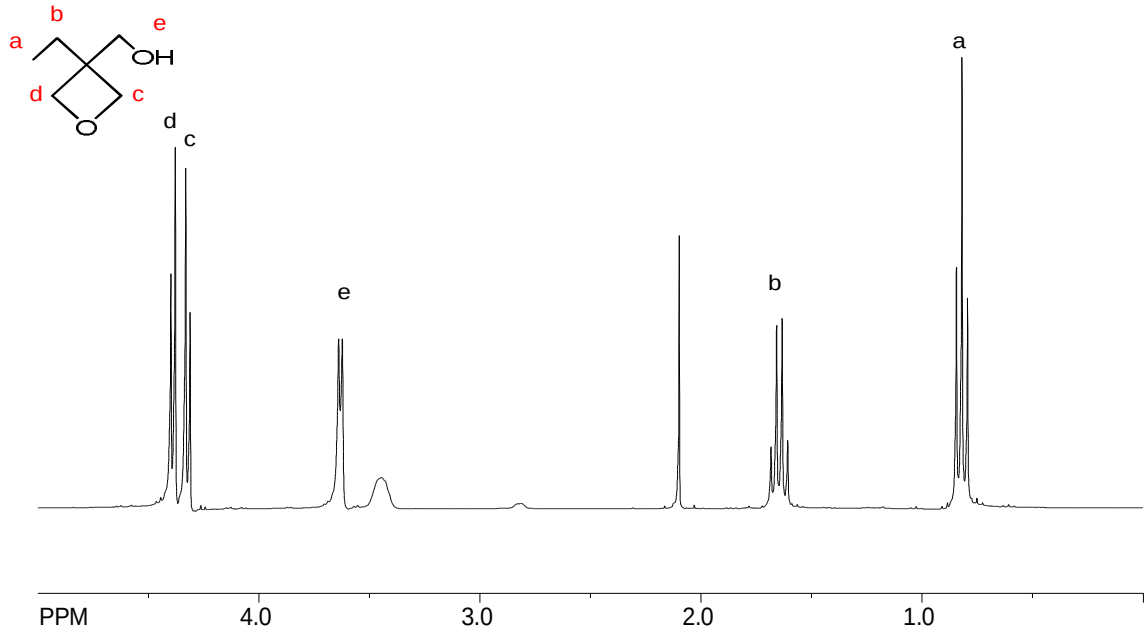

Figure 14: NMR spectra of different polymeric ratios

A) ^{13}C-NMR spectrum of poly(EHMO-EHMO$_{PEG2000}$)$_{98.2:1.8}$

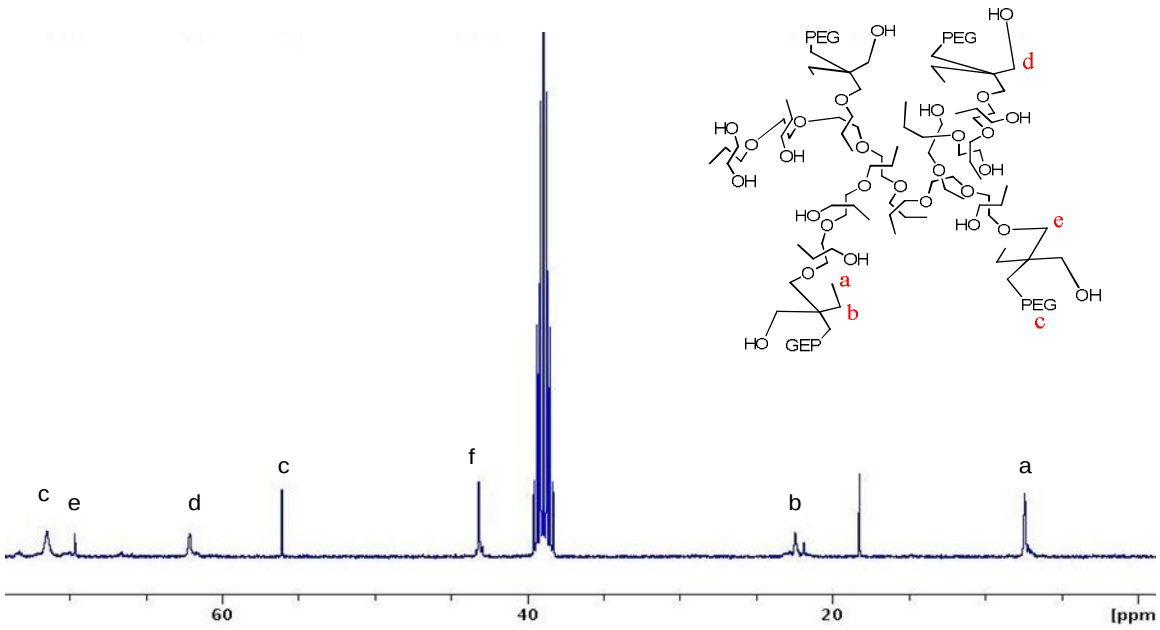

B) ^{1}H-NMR spectrum of poly(EHMO-EHMO$_{PEG2000}$)$_{98.2:1.8}$

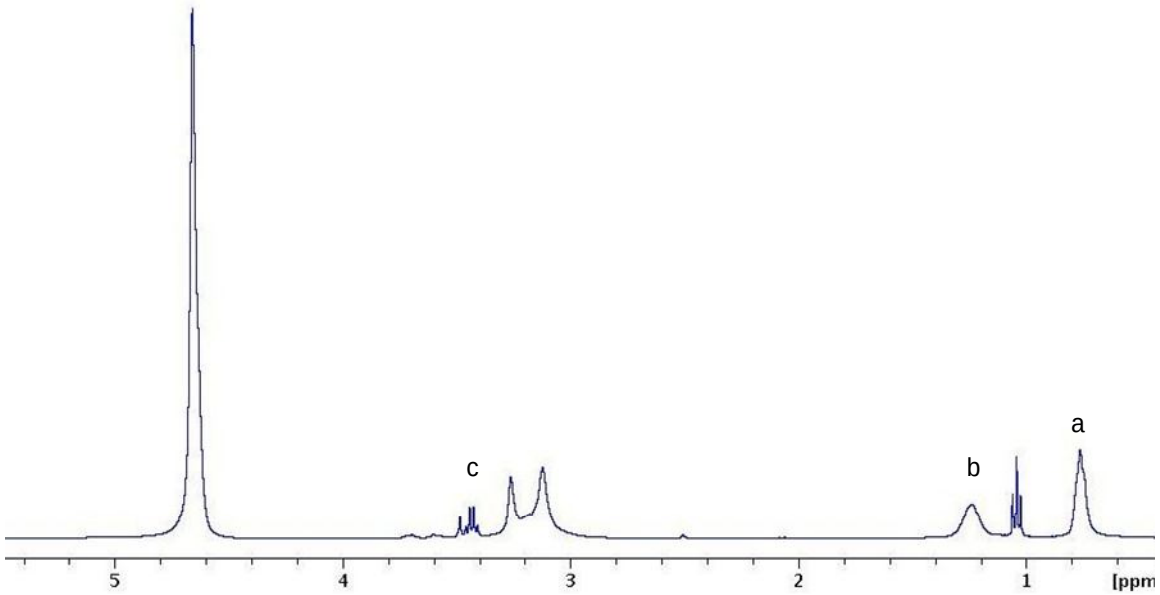

C) ^{13}C-NMR spectrum of poly(EHMO-EHMO$_{PEG2000}$)$_{96:4}$

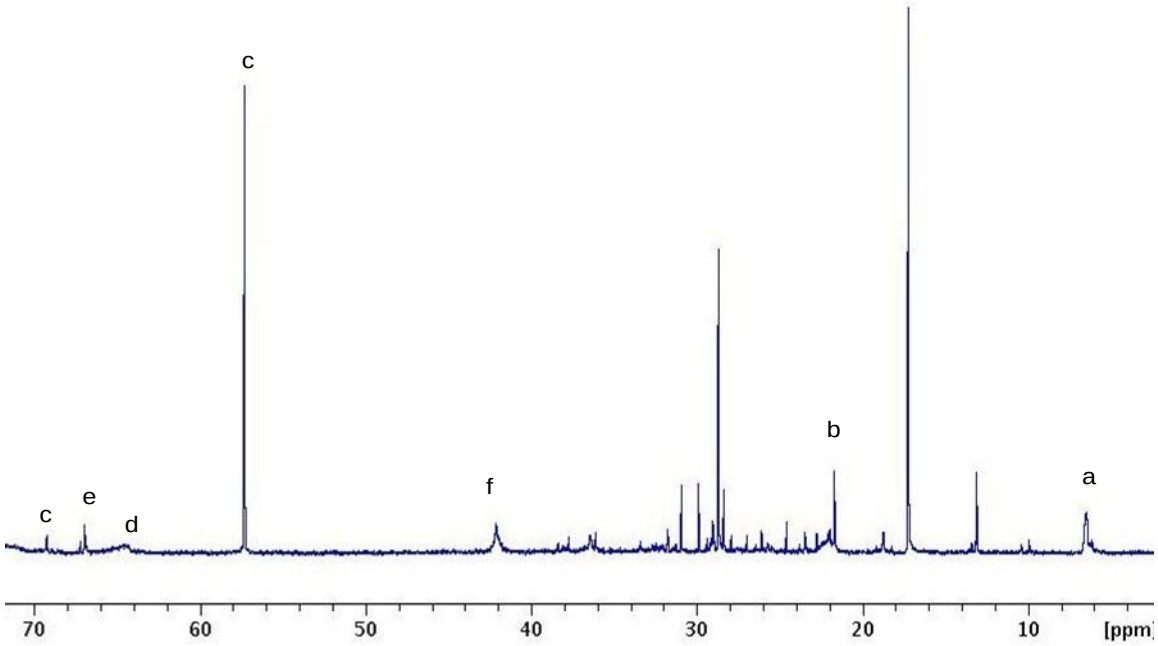

D) ^{1}H-NMR spectrum of poly(EHMO-EHMO$_{PEG2000}$)$_{96:4}$

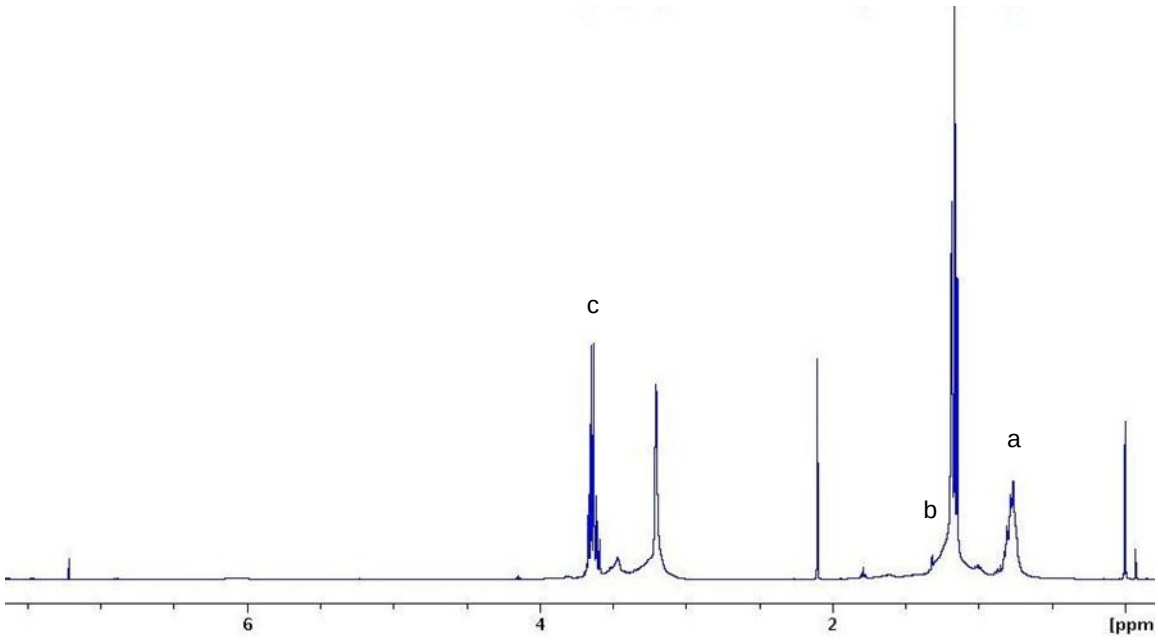

E) ^{13}C-NMR spectrum of poly(EHMO-EHMO$_{PEG2000}$)$_{74.4:25.6}$

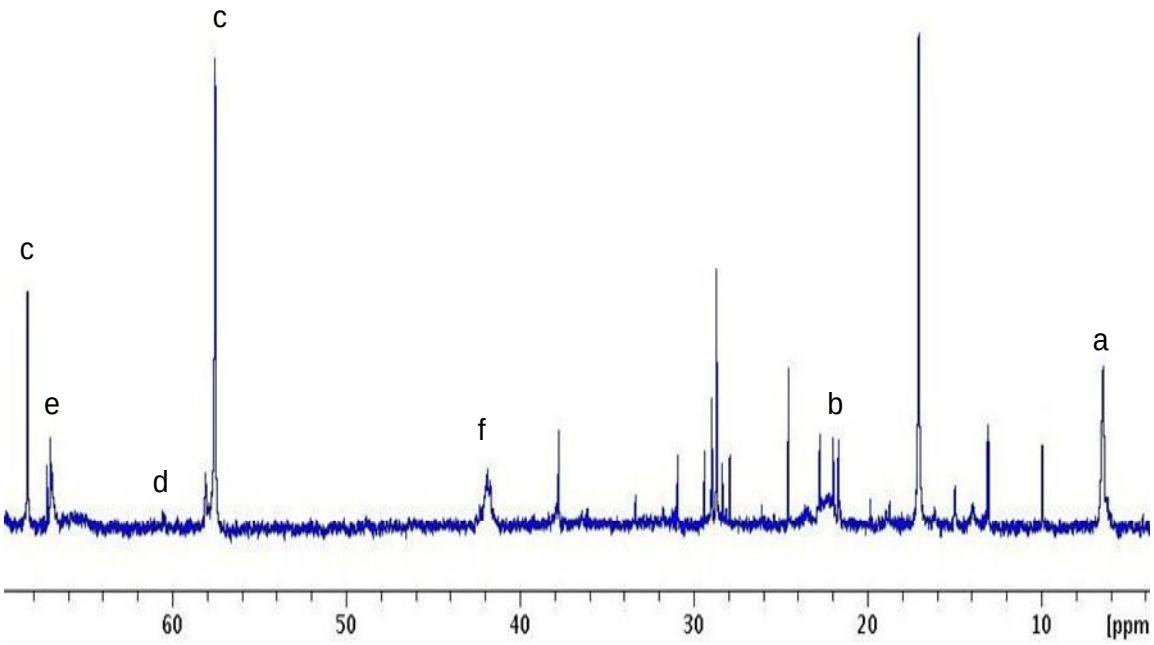

F) ^{1}H-NMR spectrum of poly(EHMO-EHMO$_{PEG2000}$)$_{74.4:25.6}$

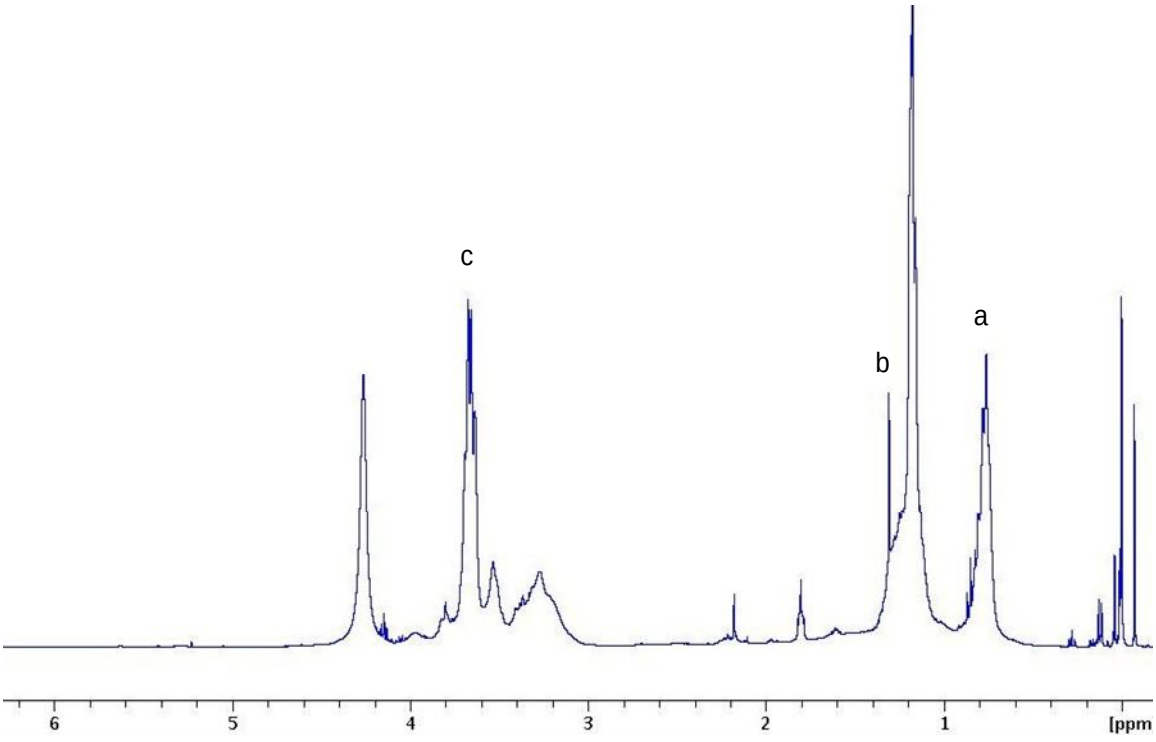

G) ^{13}C-NMR spectrum of poly(EHMO-EHMO$_{PEG550}$)$_{17:83}$

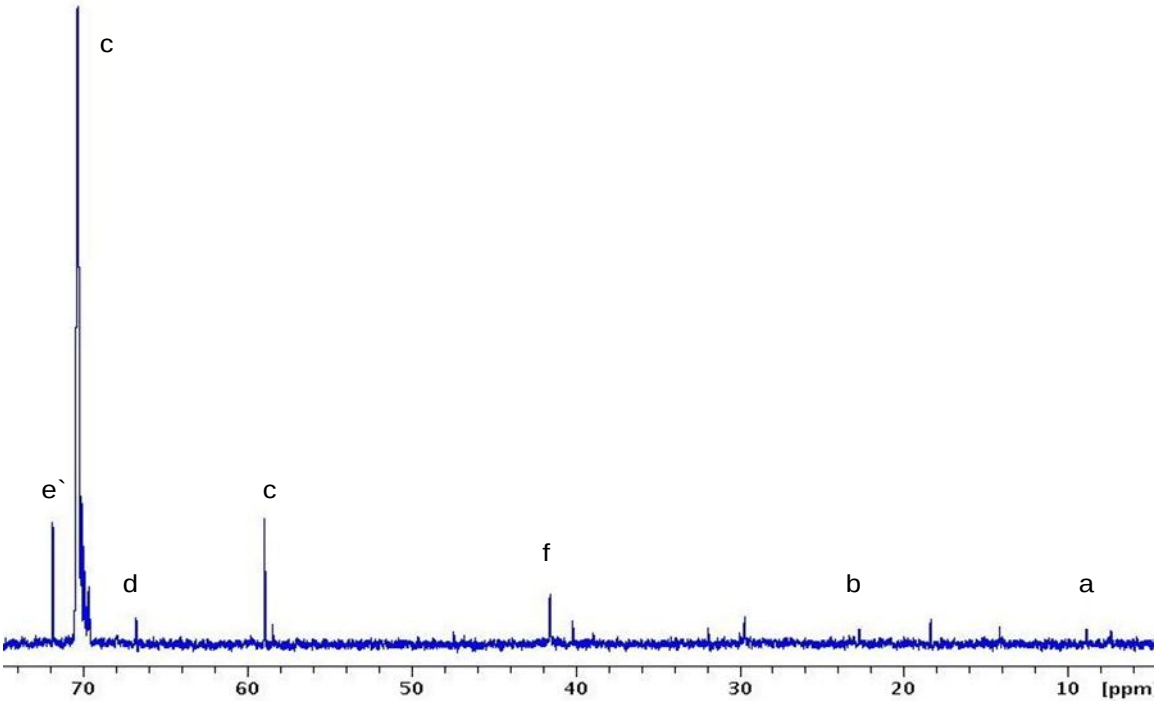

H) ^{1}H-NMR spectrum of poly(EHMO-EHMO$_{PEG550}$)$_{17:83}$

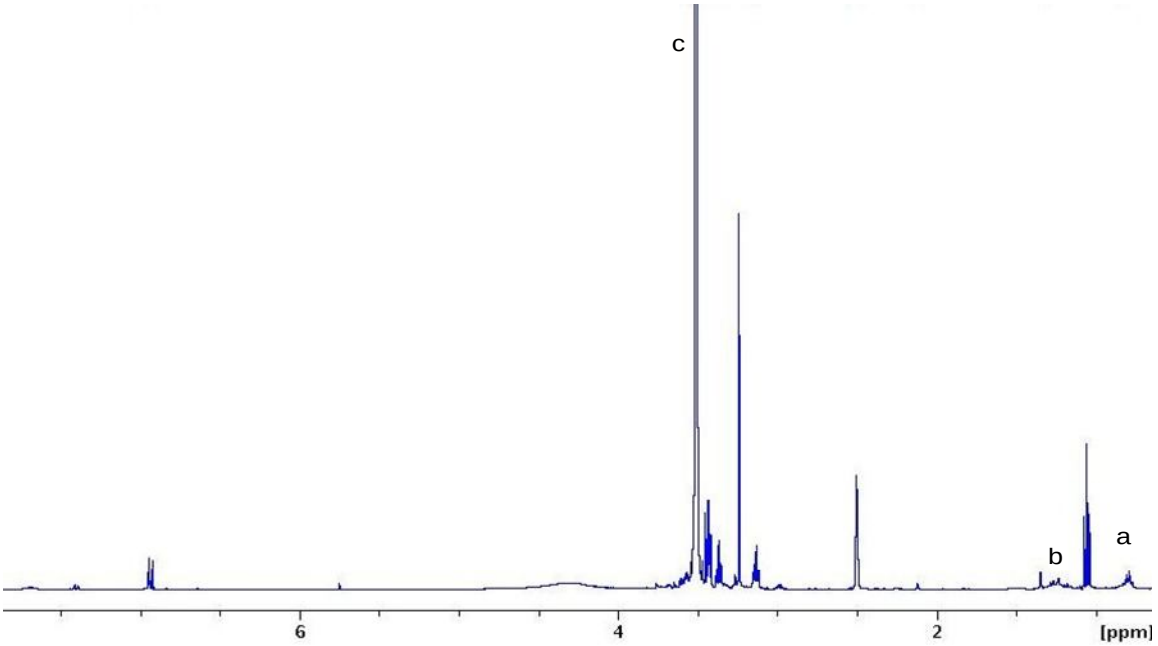

4.2 Degree of branching

The major attraction of the polymer synthesized is its hyperbranched characteristic. We can calculate its degree of branching using the following equation:

$$DOB = (D+T)/ (D+L+T)$$

D, L, T represent the dendritic (D), linear (L) and the terminal (T) units of the hyperbranched polymer (as described earlier in Figure 8). The DOB is calculated by the integration of the peaks for the D, L and T units found around 43ppm in the carbon-13 NMR (Figure 15 A,B,C and D). Degree of branching obtained for various ratios is shown in Table 7. The results indicate that the degree of branching increases with increase in monomer **2** which contributes mostly to the branches of the polymer.

Table 7: Degree of branching of various polymeric ratios

Polymer	Degree of Branching
Poly(EHMO-EHMO$_{PEG2000}$)$_{98.2:1.8}$	17.9 %
Poly(EHMO-EHMO$_{PEG2000}$)$_{96:4}$	48.47%
Poly(EHMO-EHMO$_{PEG2000}$)$_{74.4:25.6}$	76.4%
Poly(EHMO-EHMO$_{PEG550}$)$_{17:83}$	78%

Figure 15: NMR spectra of Degree of branching

A) poly(EHMO-EHMO$_{PEG2000}$)$_{98.2:1.8}$

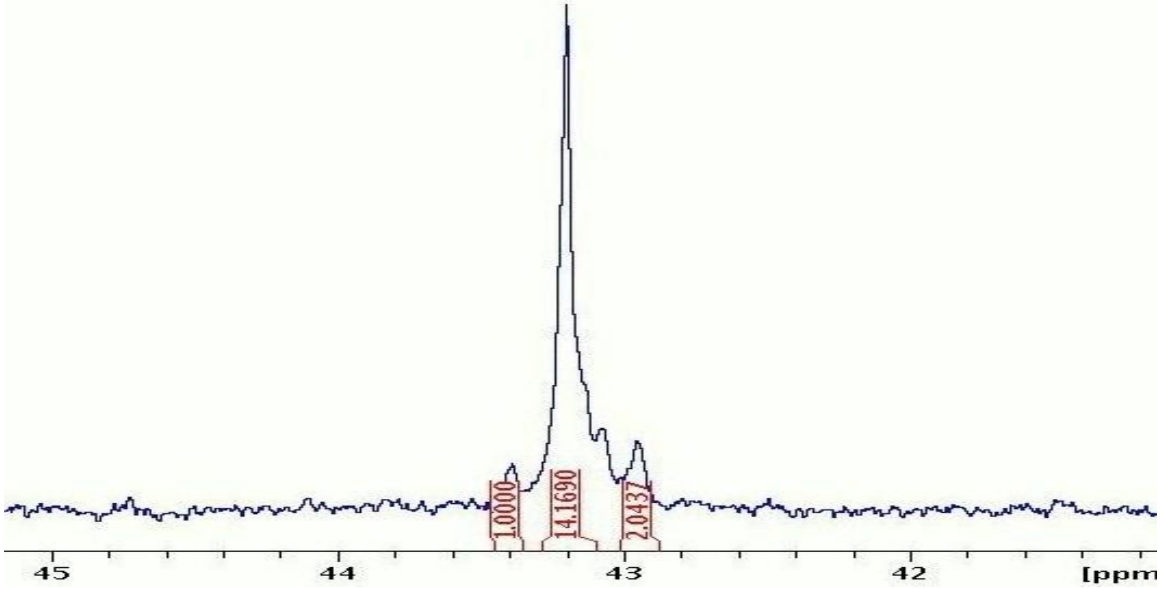

B) poly(EHMO-EHMO$_{PEG2000}$)$_{96:4}$

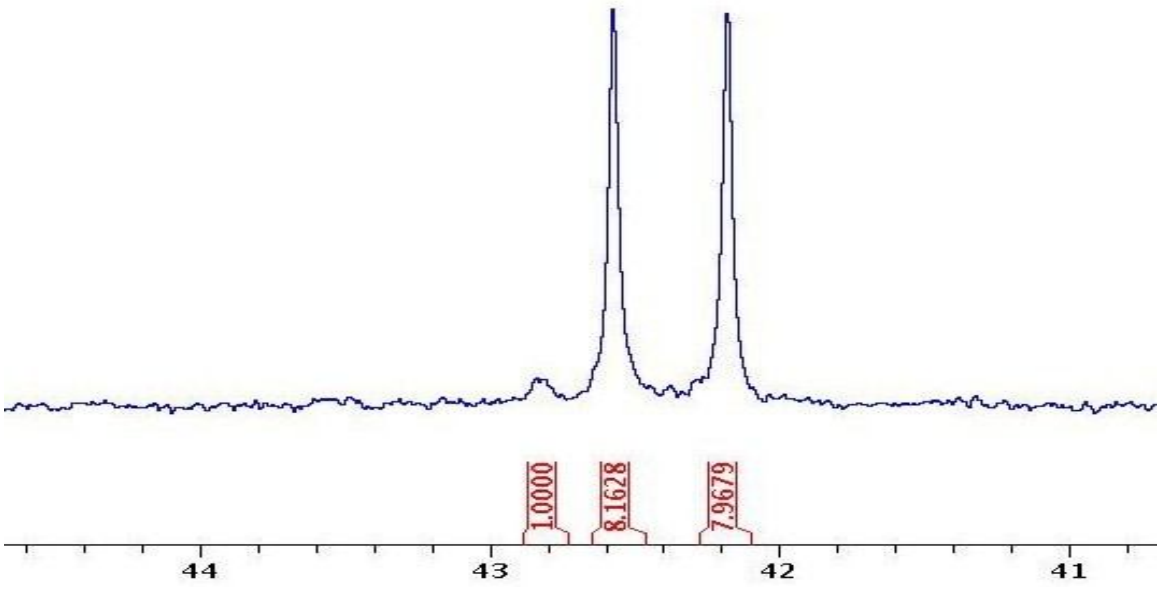

C) poly(EHMO-EHMO$_{PEG2000}$)$_{74.4:25.6}$

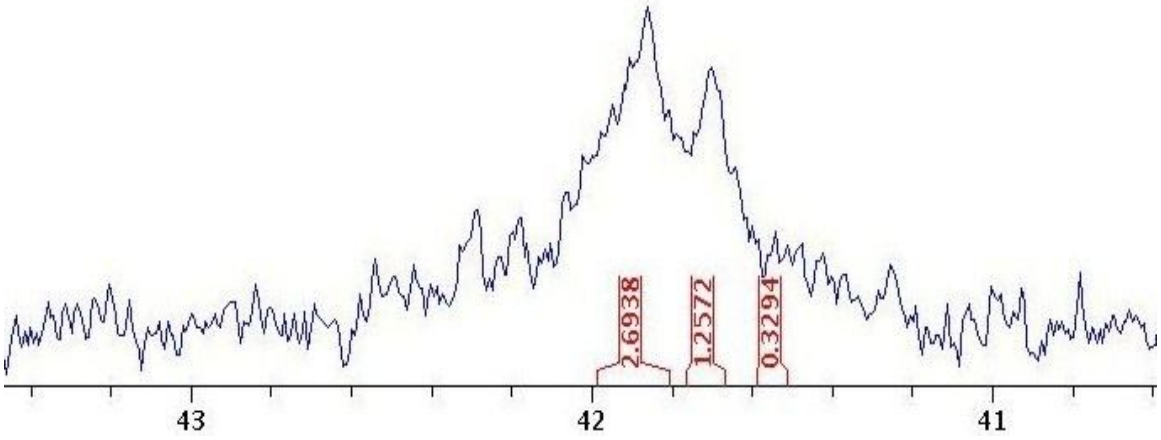

D) poly(EHMO-EHMO$_{PEG550}$)$_{17:83}$

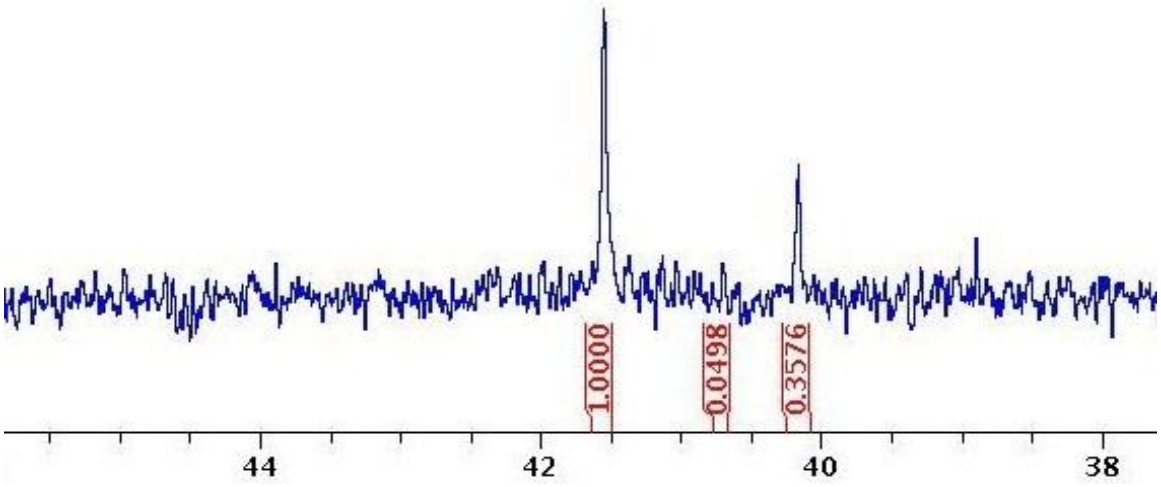

4.3 Mechanisms governing the reactions

The synthesis of the hyperbranched polymer is governed by two mechanisms known as Active Chain End mechanism (ACE) and Activated Monomer Mechanism (AMM). Polymerization is initiated by protonation of the oxygen atom in the oxetane ring which is attacked (nucleophilic) by the free hydroxyl group present on monomer **1** (EHMO). Active monomer mechanism leads to the formations of the branched core structure whereas the active chain mechanism contributes to the formation of the linear hydrophilic branches as shown in Scheme 3 below.

Scheme 3: Mechanism of polymer synthesis

A) Initiation

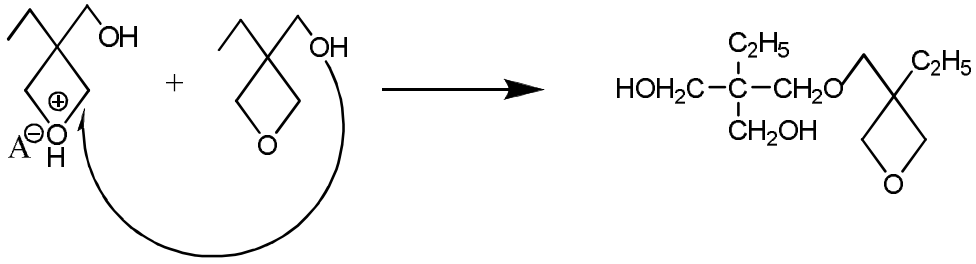

B) Propagation via AMM mechanism

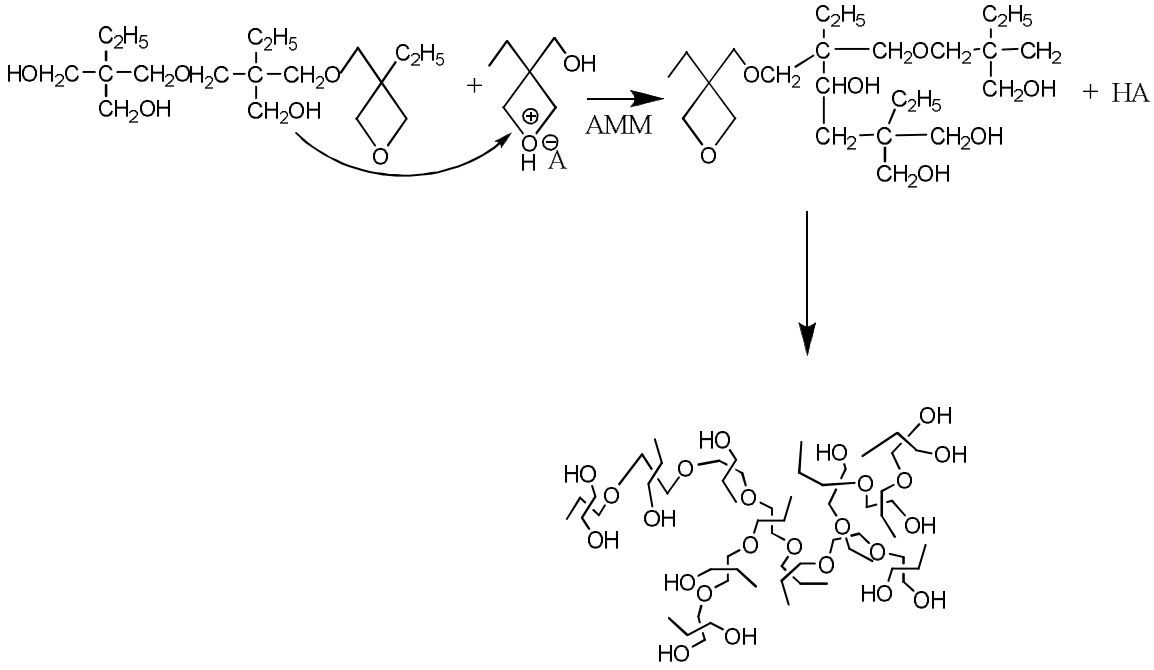

C) ACE mechanism

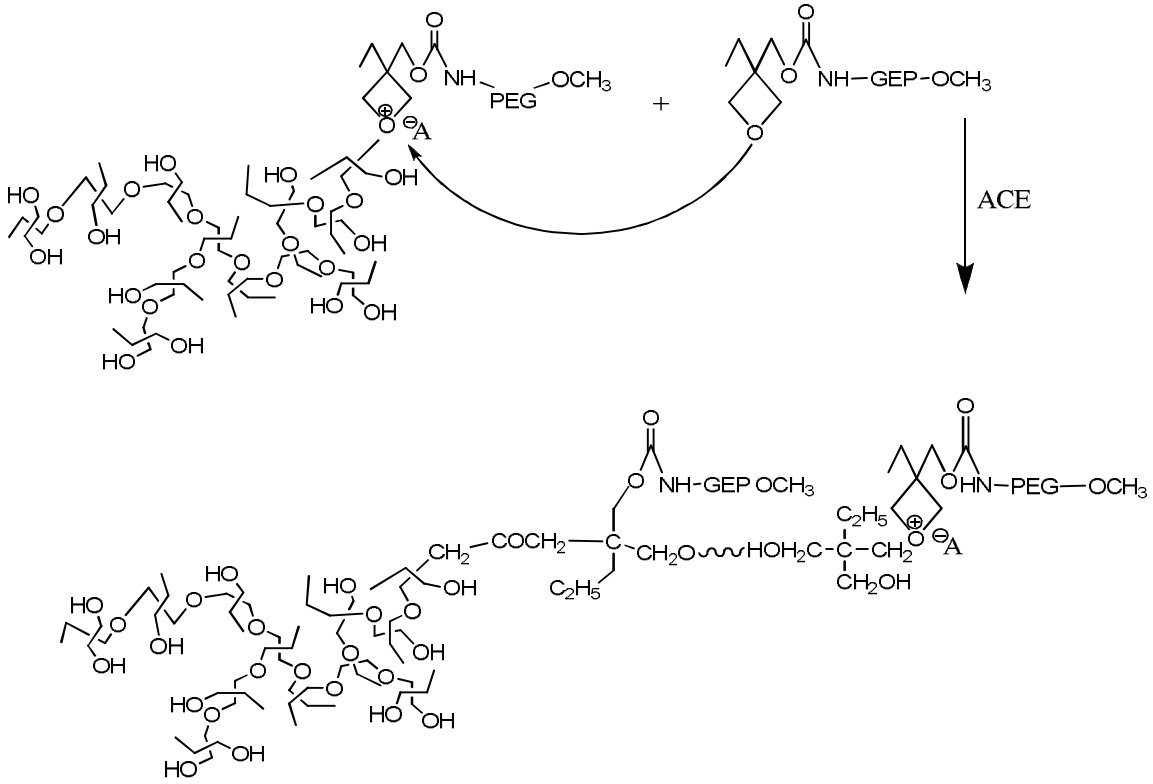

D) Termination

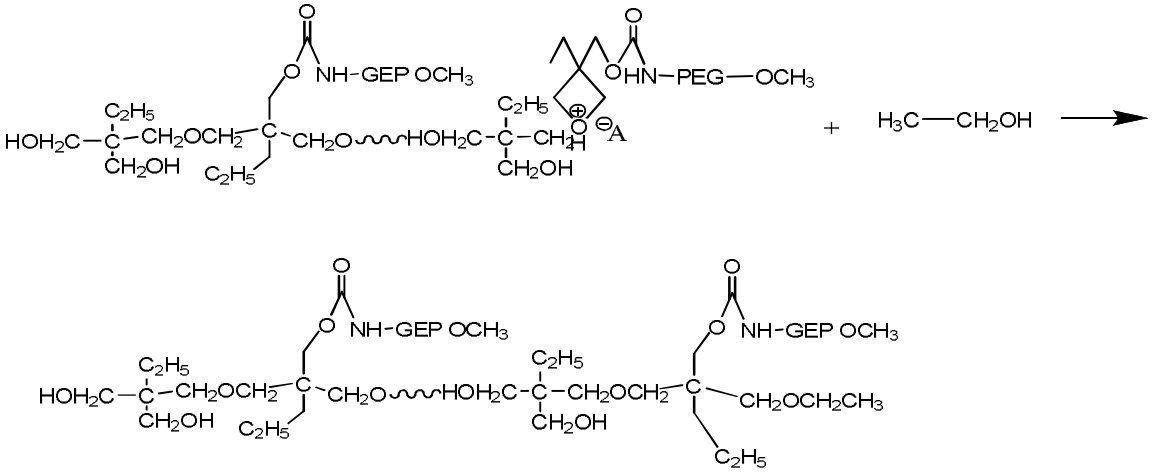

4.4 Fourier transform infrared spectroscopy

From the data obtained for FT-IR, we observed strong transmittance peaks at 2880 cm^{-1} for alkane groups, and at 1110.4 cm^{-1} for ether groups. A stretching peak at 1740 cm^{-1} was also observed for C=O bond. The results obtained from FT-IR confirm that the polymer synthesis.

Figure 16: FT-IR plots for different polymeric ratios

A) Poly(EHMO-EHMO$_{PEG2000}$)$_{98.2:1.8}$

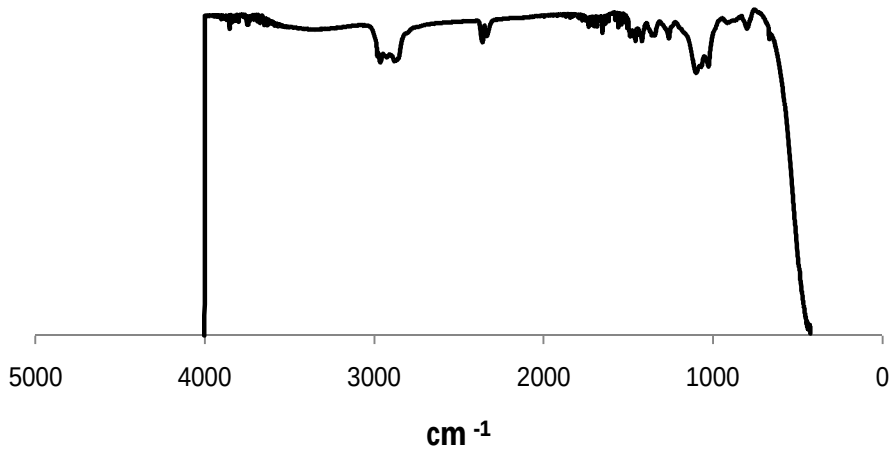

B) Poly(EHMO-EHMO$_{PEG2000}$)$_{96:4}$

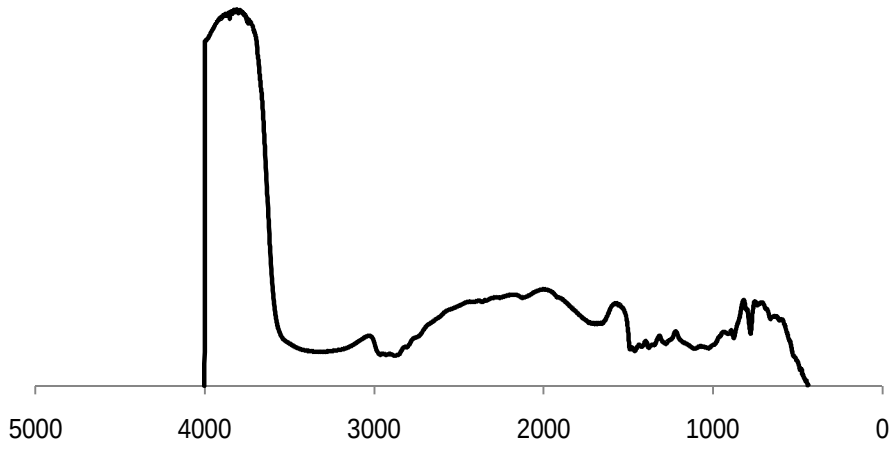

C) Poly(EHMO-EHMO$_{PEG2000}$)$_{74.4:25.6}$

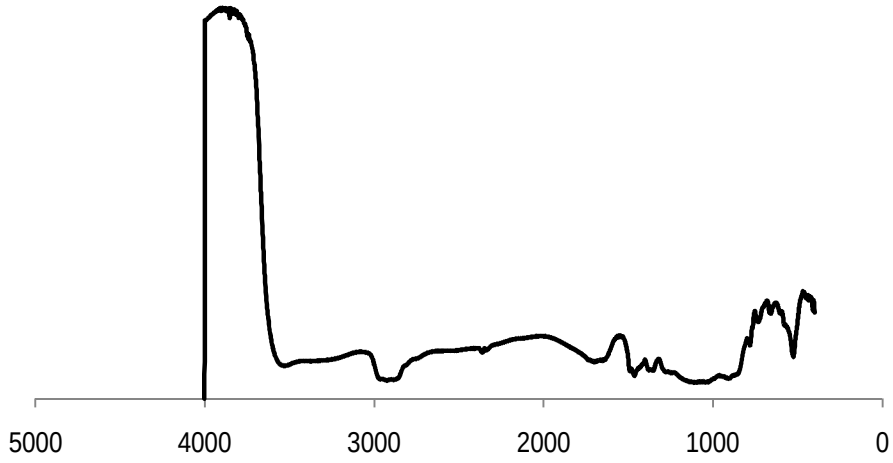

D) Poly(EHMO-EHMO$_{PEG550}$)$_{17:83}$

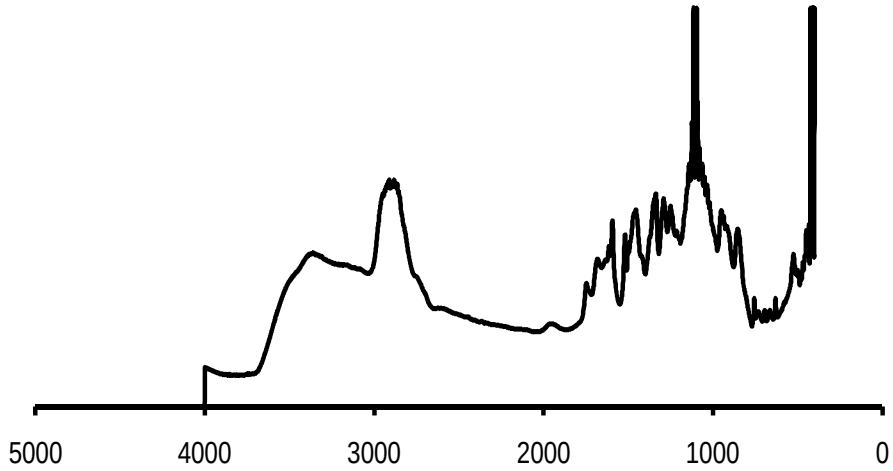

4.5 Differential scanning calorimeter

Thermal transitions were studied using differential scanning calorimetry. Glass transition temperatures were recorded as shown in Table 8. The glass transition temperature decreased with increase in the degree of branching. Glass transition temperature is influenced by free volume available for the motion of the chains and free chain ends.[38] PEG chains have a low T_g at -32 °C due to which the values for T_g keeps on decreasing as the amount of monomer **2** which has a PEG chain attached to it increases.

Table 8: Glass transition temperatures

Polymer	Glass transition temperature
Poly(EHMO-EHMO$_{PEG2000}$)$_{98.2:1.8}$ (a)	-31.5 °C
Poly(EHMO-EHMO$_{PEG2000}$)$_{96:4}$ (b)	-53.5 °C
Poly(EHMO-EHMO$_{PEG2000}$)$_{74.4:25.6}$ (c)	-43.5 °C
Poly(EHMO-EHMO$_{PEG550}$)$_{17:83}$ (d)	-55.5 °C

Figure 17: DSC curves

A) poly(EHMO-EHMO$_{PEG2000}$)$_{98.2:1.8}$

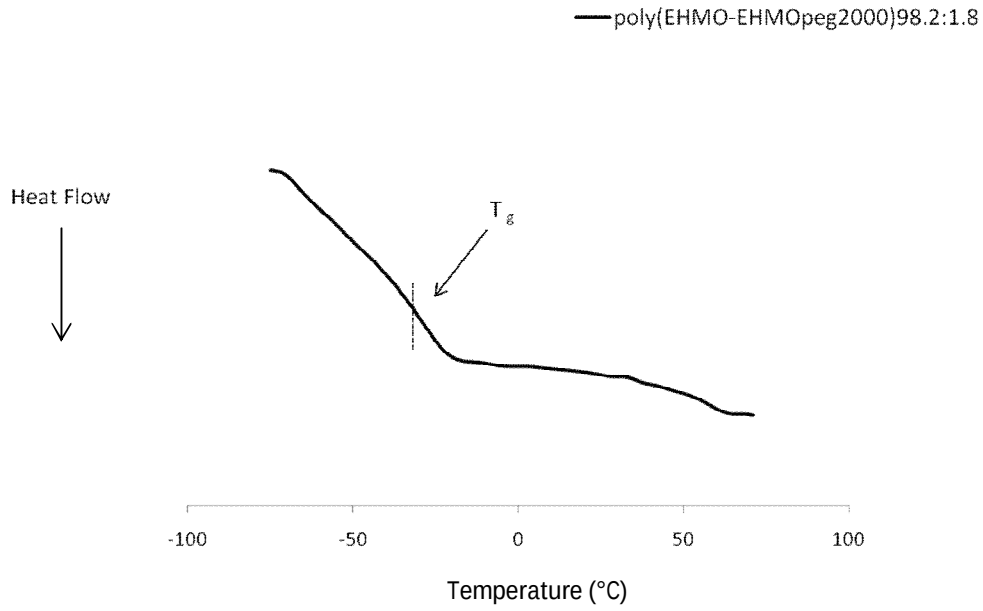

B) poly(EHMO-EHMO$_{PEG2000)\ 96:4}$

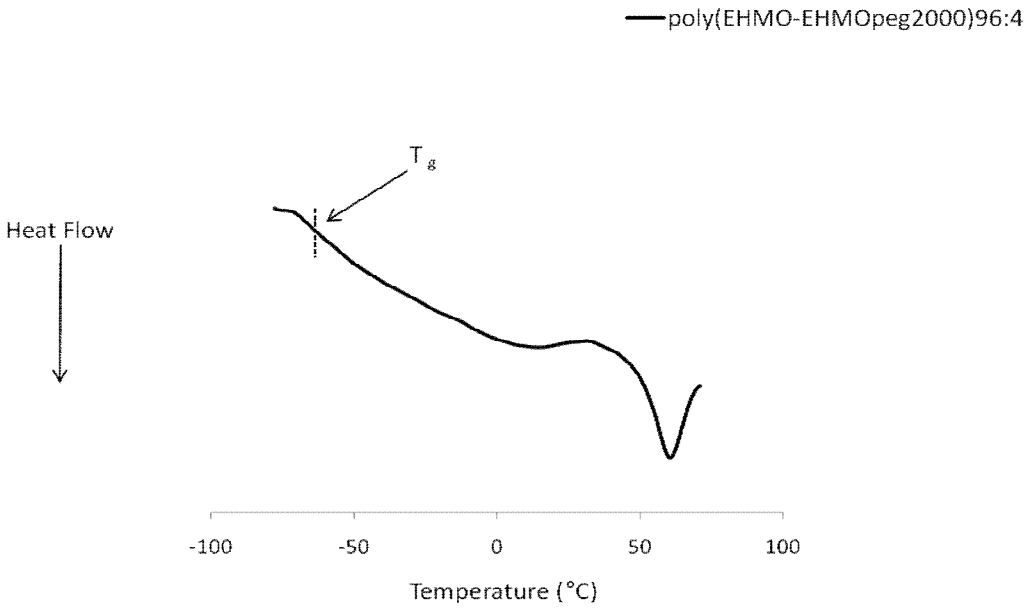

C) poly(EHMO-EHMO $_{PEG2000}$)74.5:25.6

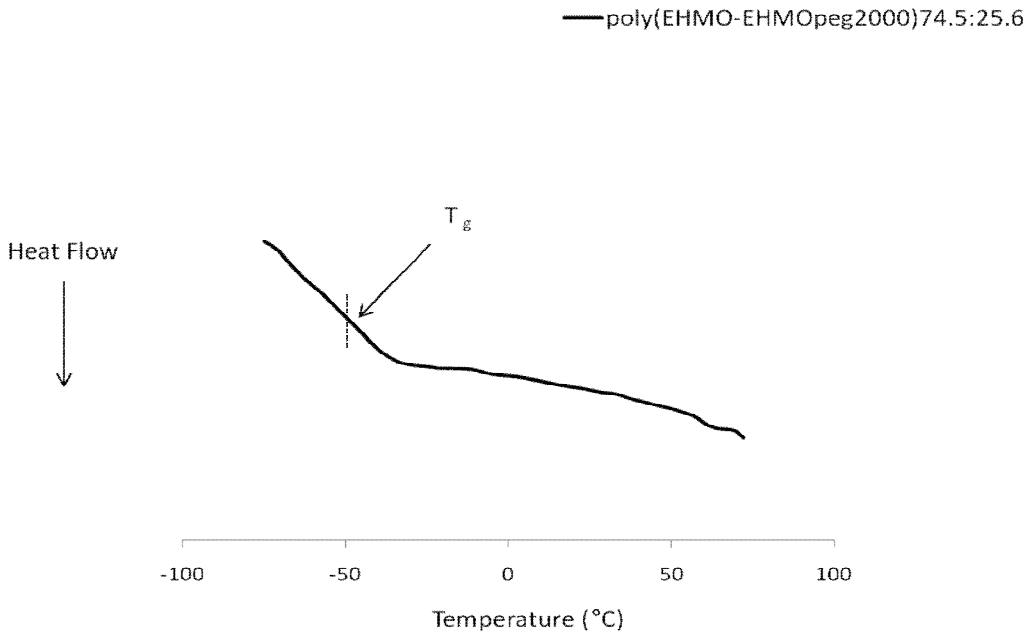

D) poly(EHMO-EHMO$_{PEG550}$)$_{17:83}$

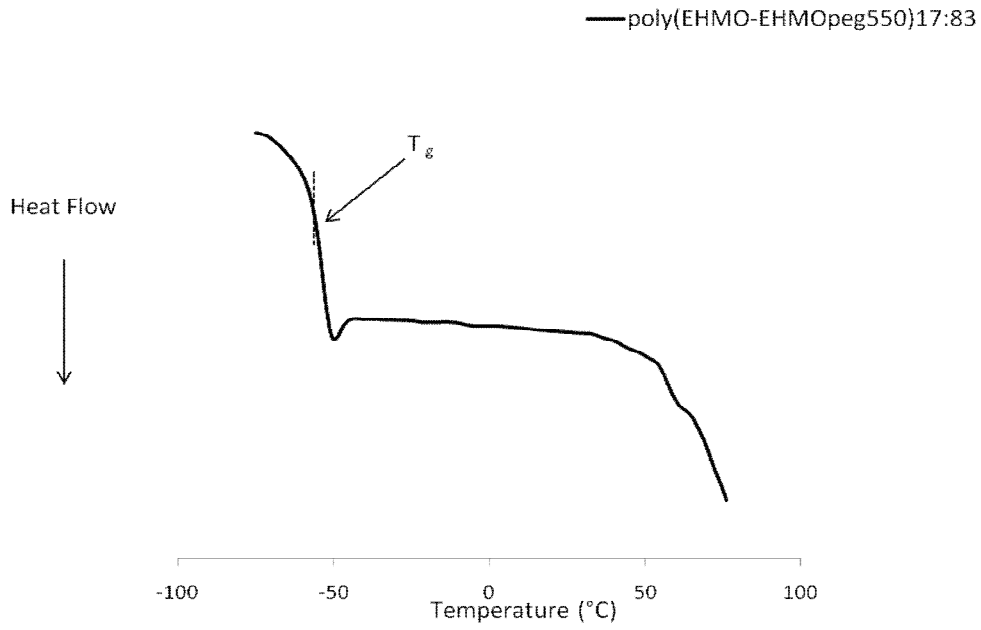

E) Combined curve for all the polymers

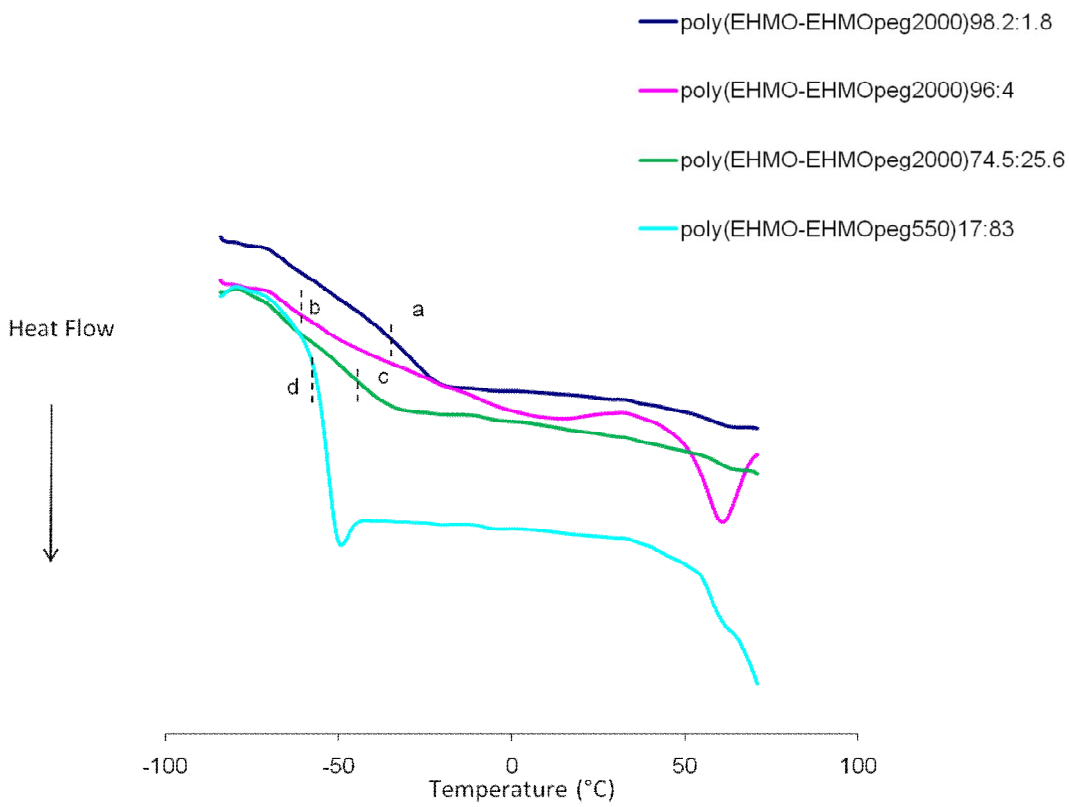

4.6 Molecular weight

Dynamic light scattering (DLS) was also used to determine the molecular weight of the polymers using toluene as the standard. The weights determined from DLS were as shown in Table 9. The results show that the molecular weight keeps increasing as the degree of branching and amount of monomer **2** increases.

Table 9: Molecular weight determined from DLS

Polymer	Molecular weight
Poly(EHMO-EHMO$_{PEG2000}$)$_{98.2:1.8}$	20.96 kDa
Poly(EHMO-EHMO$_{PEG2000}$)$_{96:4}$	28.1 kDa
Poly(EHMO-EHMO$_{PEG2000}$)$_{74.4:25.6}$	34.34 kDa
Poly(EHMO-EHMO$_{PEG550}$)$_{17:83}$	7.8 kDa

4.7 Preparation of polymeric particles

Both blank and drug loaded nanoparticles were prepared by the method described earlier and their morphology and size were characterized using SEM (scanning electron microscopy) and DLS (dynamic light scattering). SEM images (Figure 18) shows that the particles were mostly circular in shape and the diameter ranged from 200 nm to 500 nm depending upon the copolymer composition. The spherical shape of the particles was

maintained after the drug was encapsulated. DLS was also used to provide quantitative size information. The size of polymeric particles obtained from DLS ranged between 250 nm and 700 nm and were found to be consistent with the SEM results. The difference in size measured by both techniques was possibly due to the method by which the samples were prepared for SEM. Since the samples were obtained by putting a few drops of the solution on silicon wafers and then drying them in the vacuum oven for 4-6 hours, there is a possibility that the drying might have caused the shrinkage of the particles.[23, 25] The size of the drug loaded particles was bigger than that of the blank particles indicating the encapsulation of the drug into the particles as shown in the Figure 19.

Table 10: Particle size determined using DLS and SEM

Blank particle sizes	DLS (nm)	SEM (nm)
Poly(EHMO-$EHMO_{PEG2000}$)$_{98.2:1.8}$	685.5 ± 5.25	450-550
Poly(EHMO-$EHMO_{PEG2000}$)$_{96:4}$	509 ± 5.50	480-450
Poly(EHMO-$EHMO_{PEG2000}$)$_{74.4:25.6}$	361 ± 7.20	150-200
Poly(EHMO-$EHMO_{PEG550}$)$_{17:83}$	1078 ± 5.60	900-1000

The particle size was found to be decreasing with increase in the amount of monomer **2** which mostly form the hydrophilic branches of the polymer. This behavior is in accordance to the Eisenberg et al. theory [42] which says that thermodynamics of aggregation governs the size of the micelles. They proposed three sources which may influence the behavior of micelles namely, the core, core-solvent interaction, and shell-solvent interaction.

Figure 18: SEM images of blank polymeric particles

A) Poly(EHMO-EHMO$_{PEG2000}$)$_{98.2:1.8}$

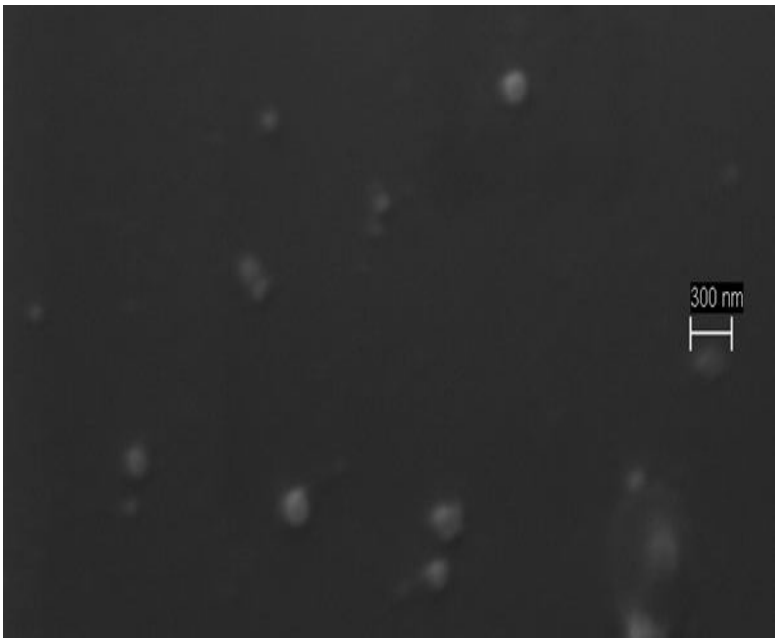

B) Poly(EHMO-EHMO$_{PEG2000}$)$_{96:4}$

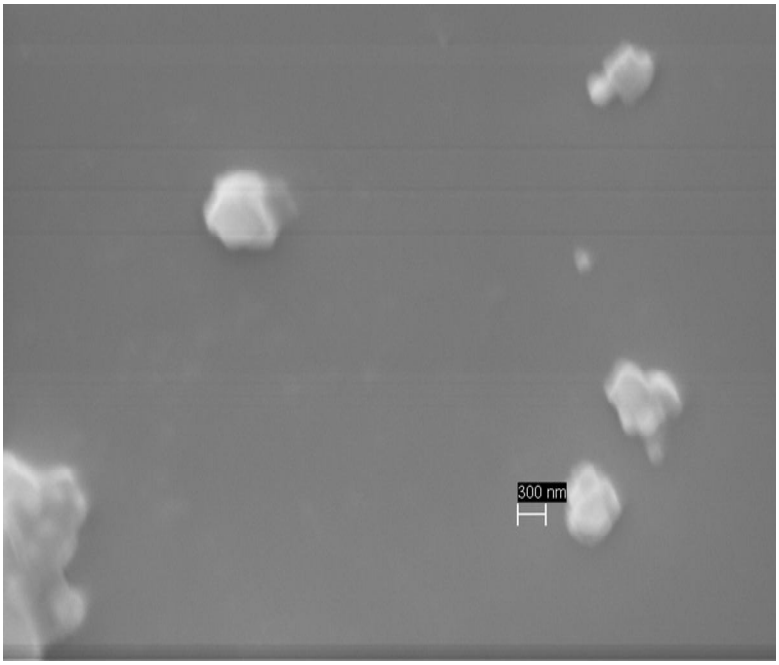

C) Poly(EHMO-EHMO$_{PEG2000}$)$_{74.4:25.6}$

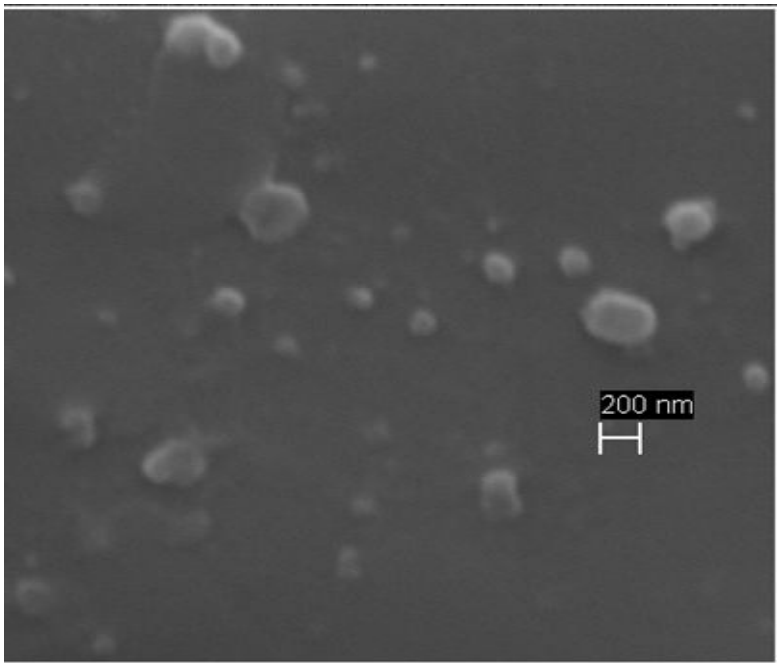

D) Poly(EHMO-EHMO$_{PEG550}$)$_{17:83}$

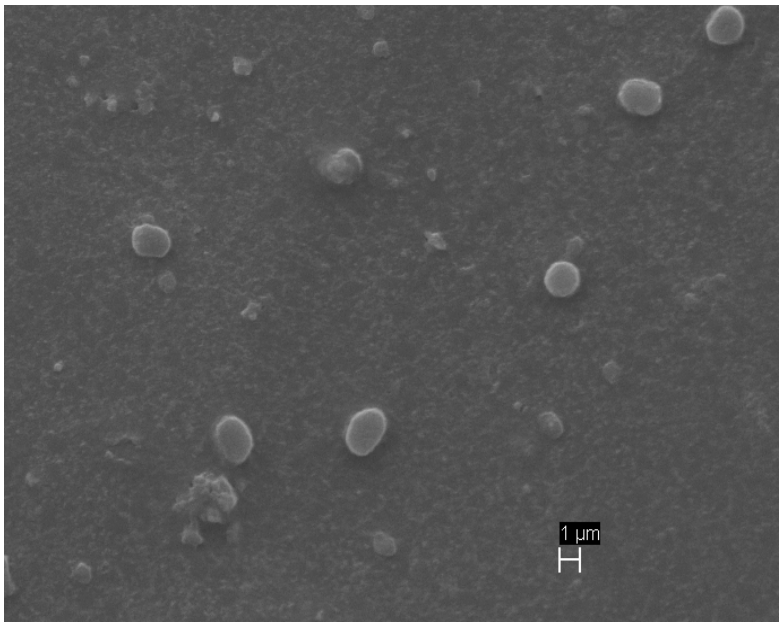

Figure 19: Comparison study between blank and drug loaded particles:

A) Poly(EHMO-EHMO$_{PEG2000}$)$_{98.2:1.8}$

Before drug encapsulation

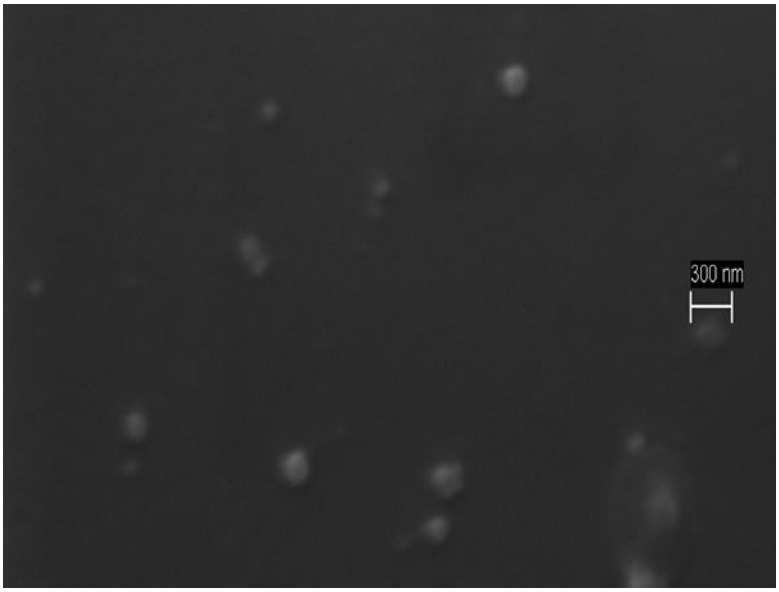

After drug encapsulation

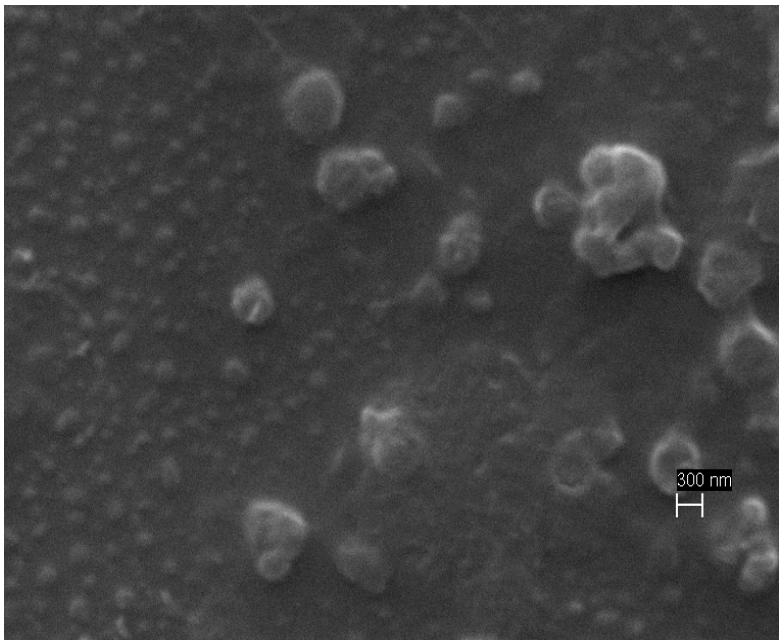

B) Poly(EHMO-EHMO$_{PEG2000}$)$_{96:4}$
Before drug encapsulation

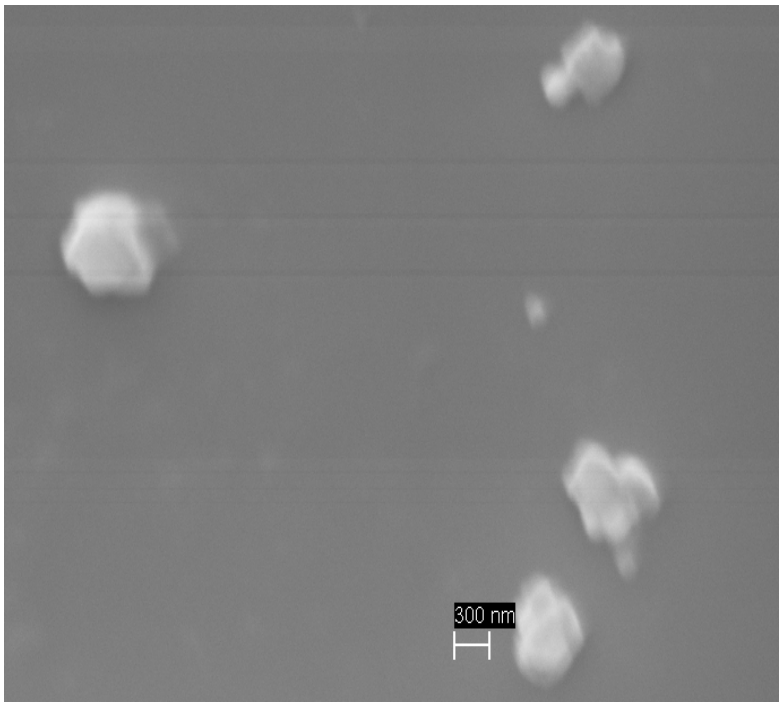

After drug encapsulation

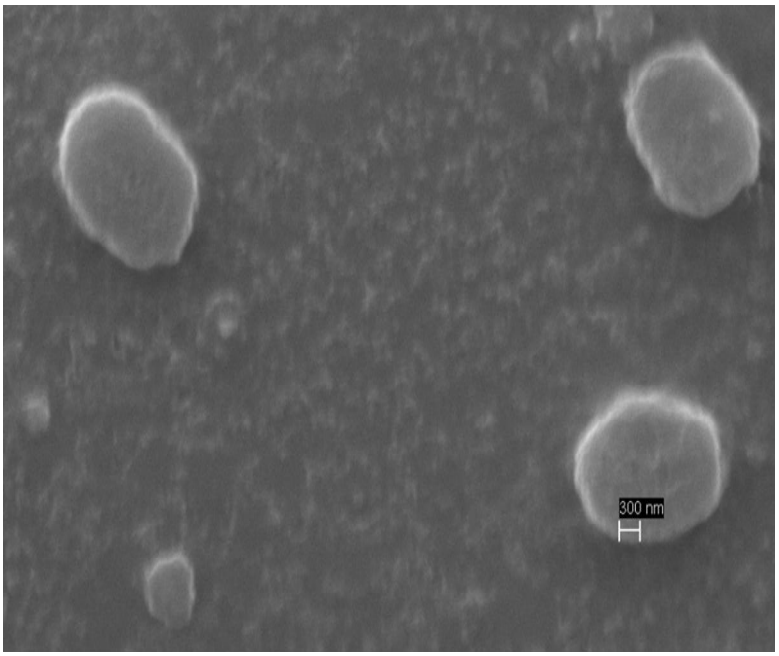

C) Poly(EHMO-EHMO$_{PEG2000}$)$_{74.4:25.6}$
Before drug encapsulation

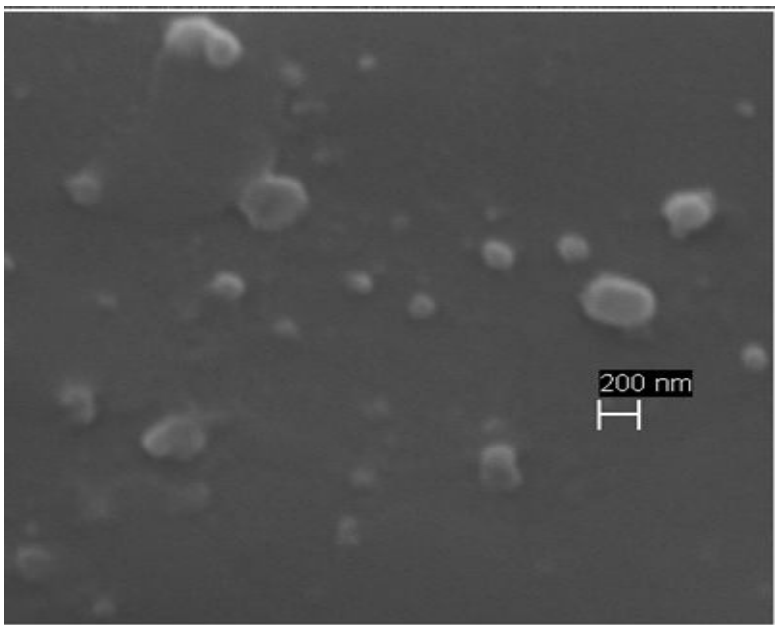

After drug encapsulation

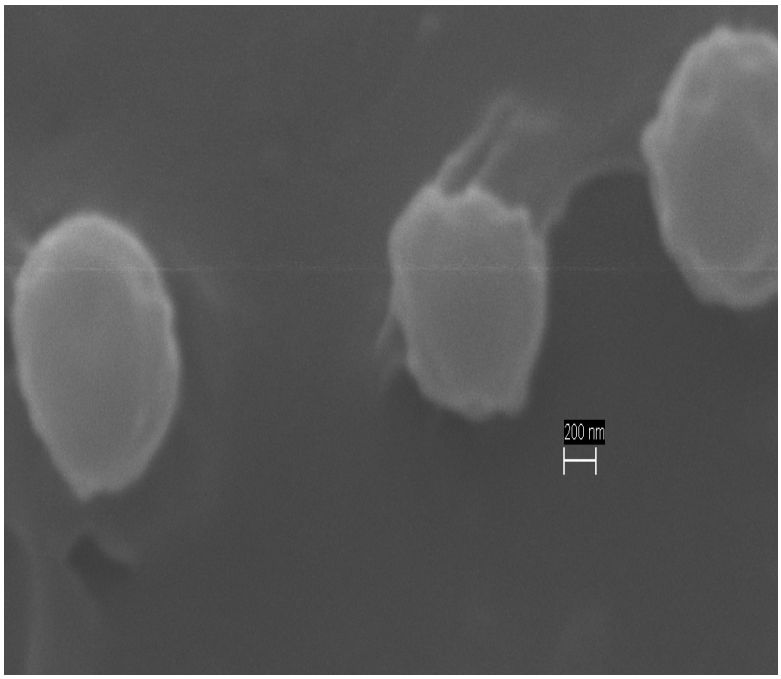

D) Poly(EHMO-EHMO$_{PEG550}$)$_{17:83}$
Before drug encapsulation

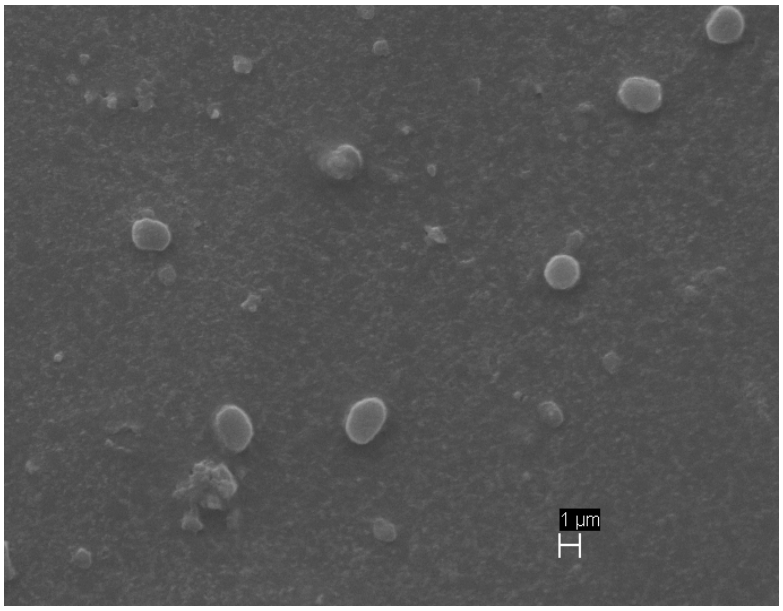

After drug encapsulation

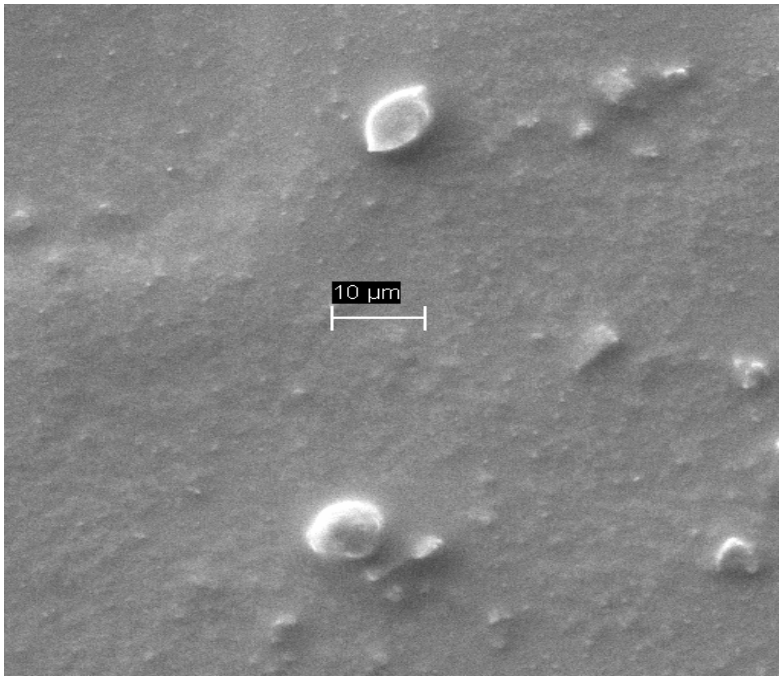

4.8 Cytotoxicity studies

Cytotoxicity tests were performed using human dermal fibroblasts cells. Positive control was used, where the fibroblast cells were incubated with zero concentration of polymer. The studies clearly indicated that addition of PEG to the polymer reduced the cytotoxicity of the material. Cell viability was the highest for the polymer with the maximum amount of PEG i.e. poly(EHMO-EHMO$_{PEG550}$)$_{17:83}$ as shown in Figure 20. Cell images (Figure 21) confirm that the cells incubated were not affected in terms of morphology. As seen in both cell viability assay and cell imaging analysis poly(EHMO-EHMO$_{PEG550}$)$_{17.83}$ was the least toxic. Figure 21 further shows the effect of increasing concentrations (from 0.01 µg/µl to 0.33 µg/µl) of different polymeric ratios on the fibroblast cells. The cytotoxicity studies suggest the cytotoxicity of the polymeric particles is dose and composition dependent.

Figure 20: Cytotoxicity studies

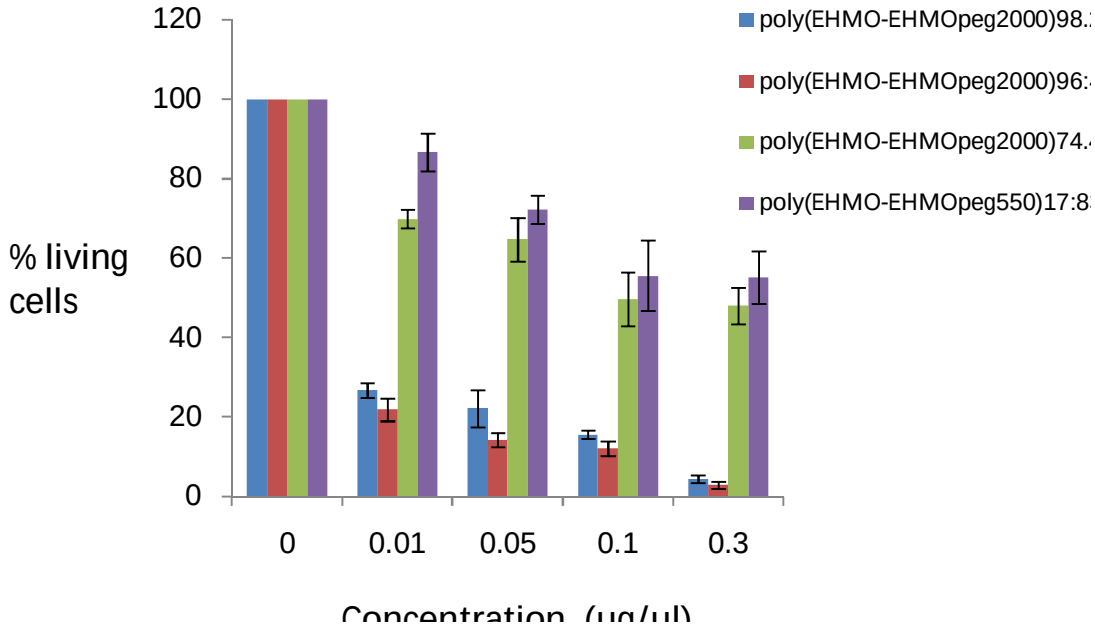

Figure 21: Microscopic images for cytotoxicity studies

A) Poly(EHMO-EHMO$_{PEG2000}$)$_{98.2:1.8}$

i) 0.01µg/µl

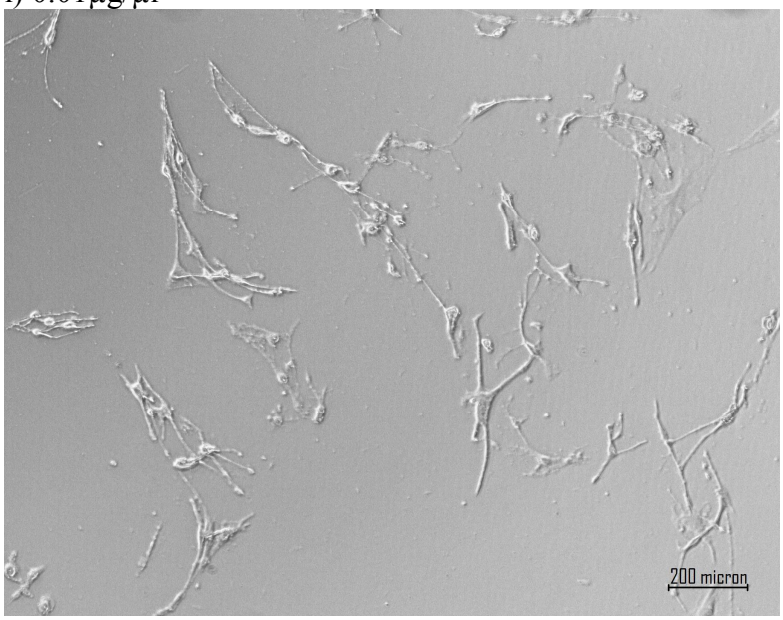

ii) 0.05µg/µl

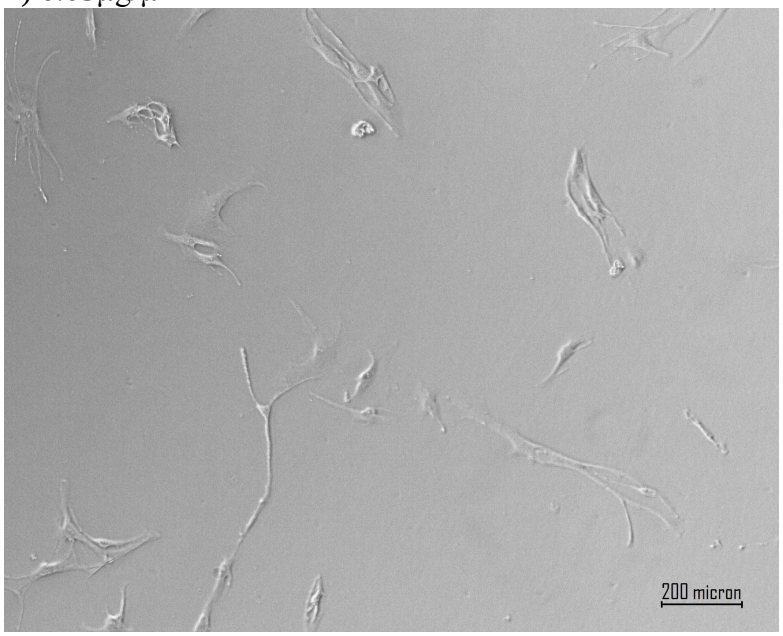

iii) 0.1µg/µl

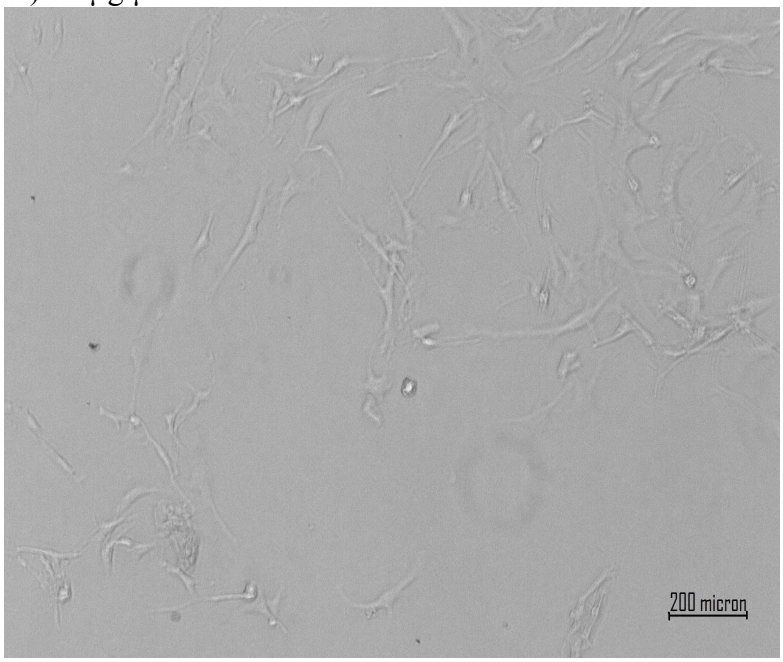

iv) 0.33µg/µl

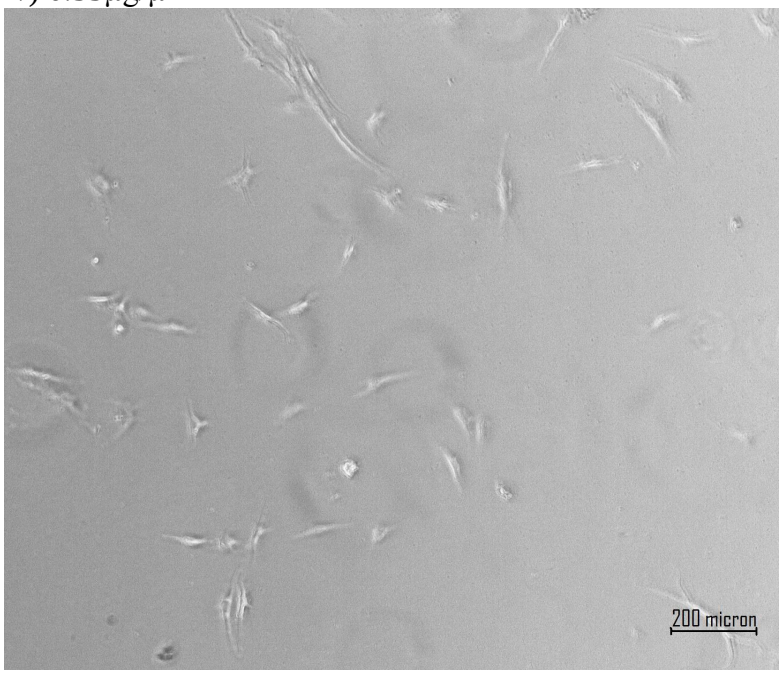

B) Poly(EHMO-EHMO$_{PEG2000}$)$_{96:4}$

i) 0.01µg/µl

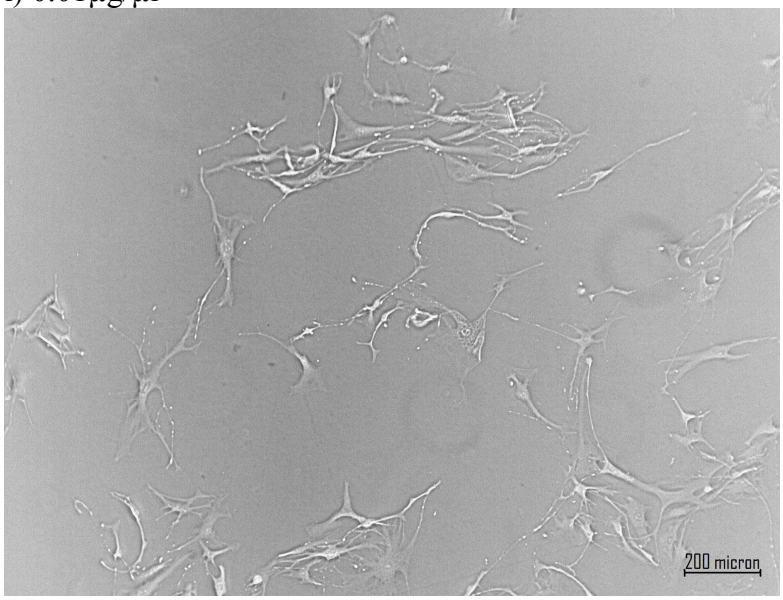

ii) 0.05µg/µl

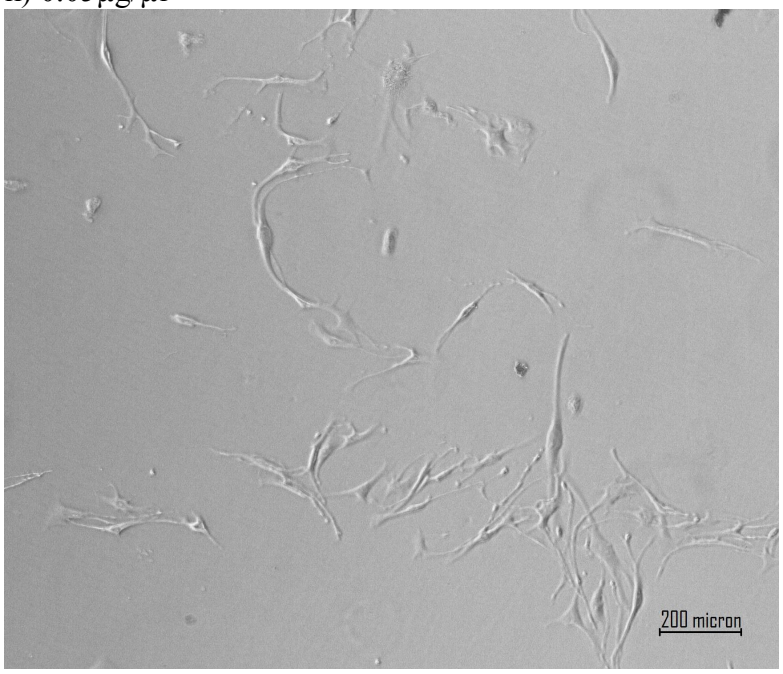

iii) 0.1µg/µl

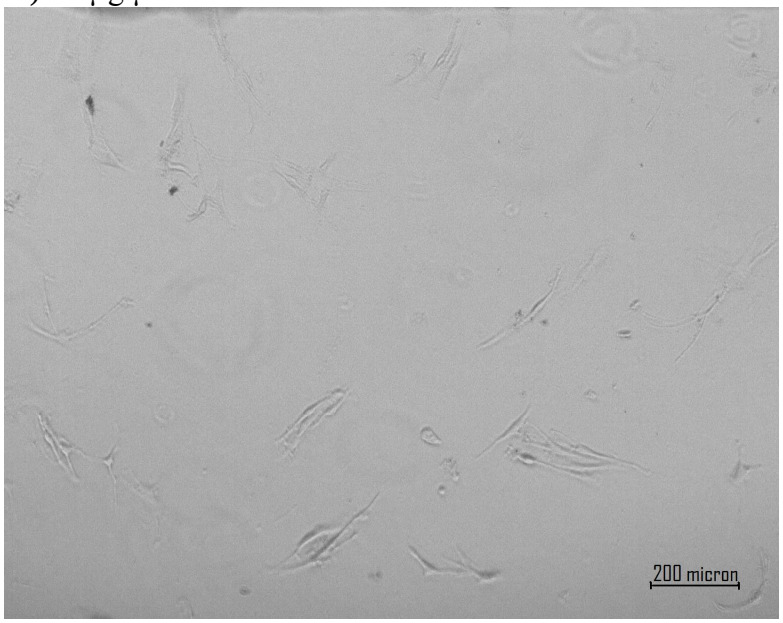

iv) 0.33µg/µl

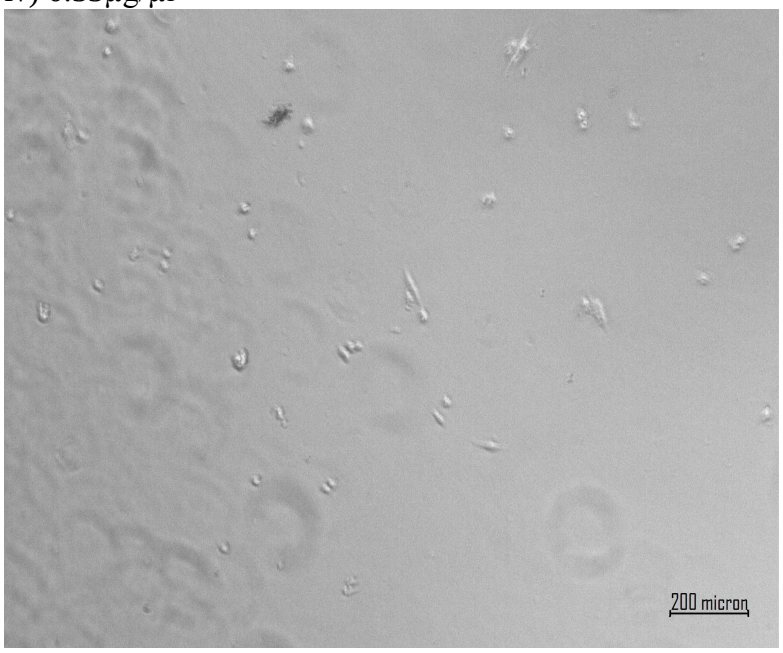

C) Poly(EHMO-EHMO$_{PEG2000}$)$_{74.4:25.6}$

i) 0.01µg/µl

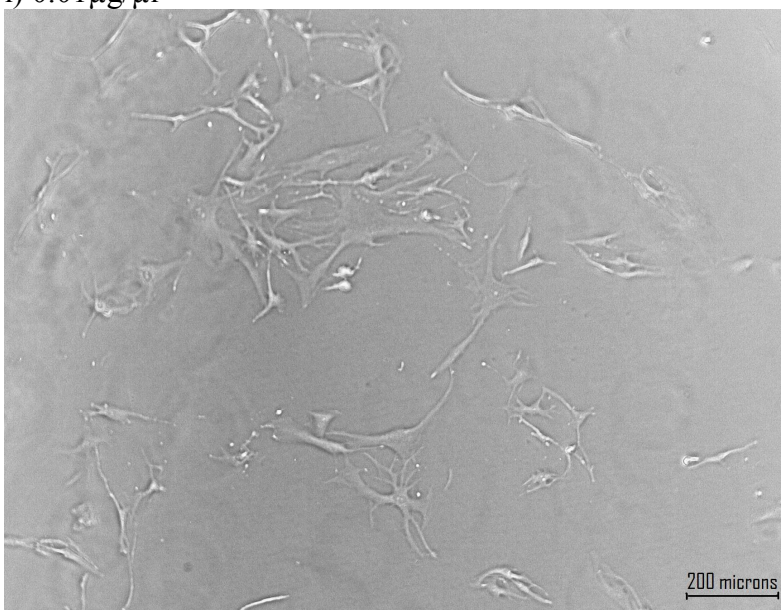

ii) 0.05µg/µl

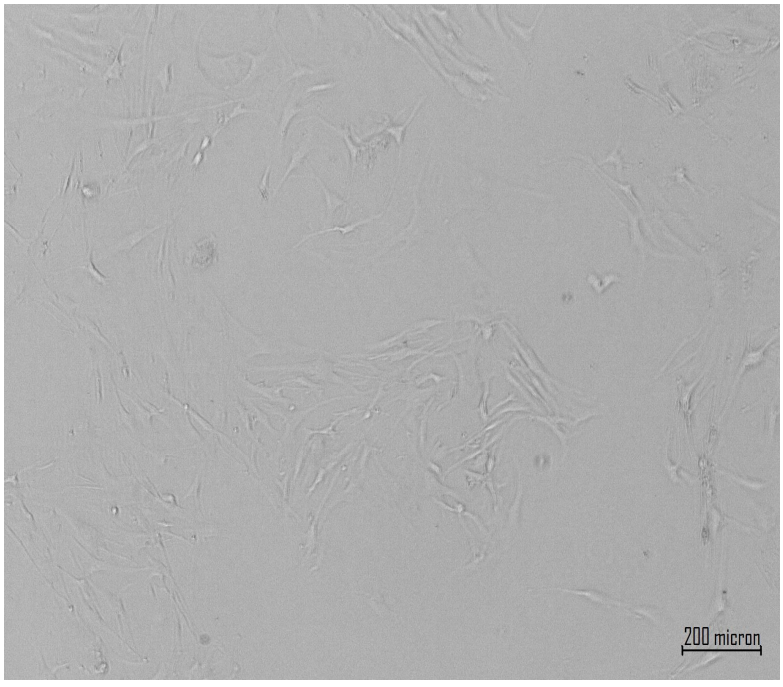

iii) 0.1µg/µl

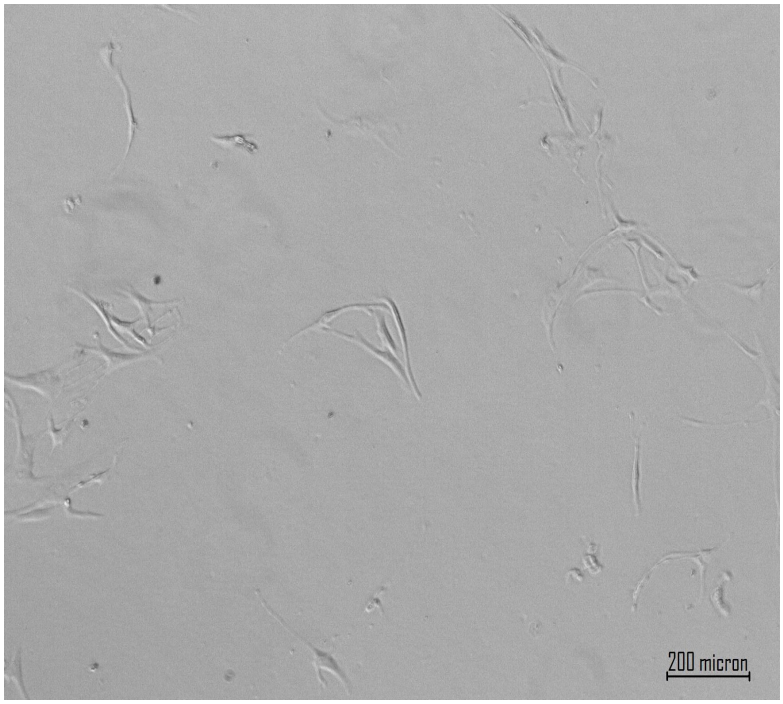

iv) 0.33µg/µl

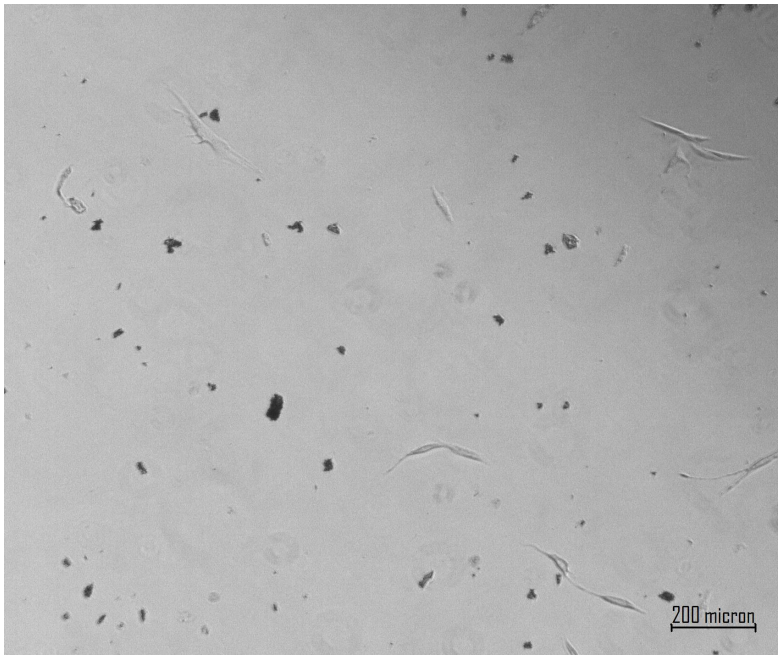

D) Poly(EHMO-EHMO$_{PEG550}$)$_{17:83}$

i) 0.01µg/µl

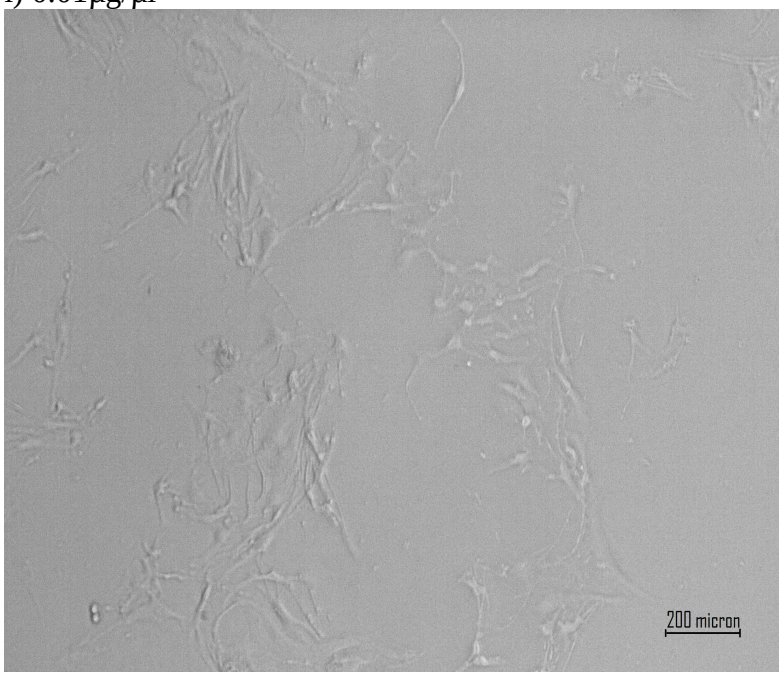

ii) 0.05µg/µl

iii) 0.1µg/µl

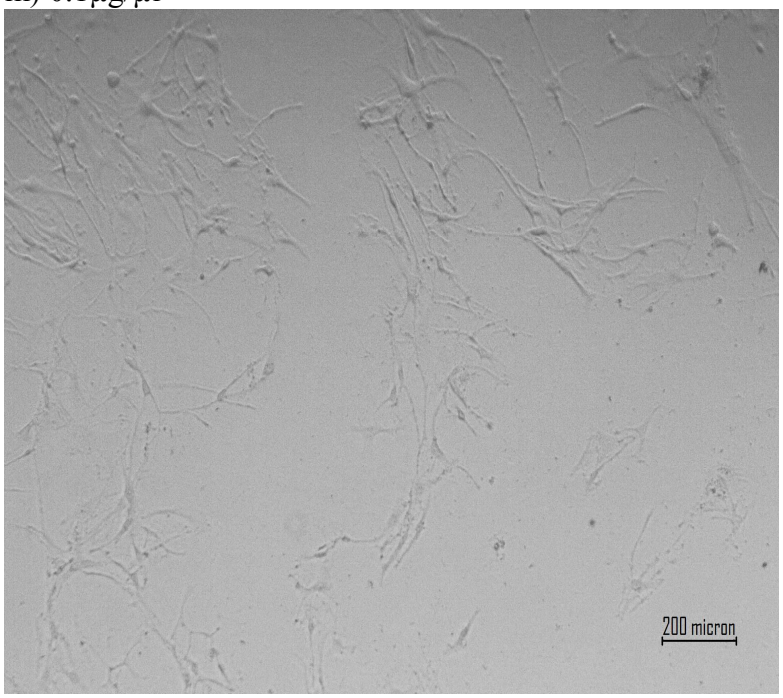

iv) 0.33µg/µl

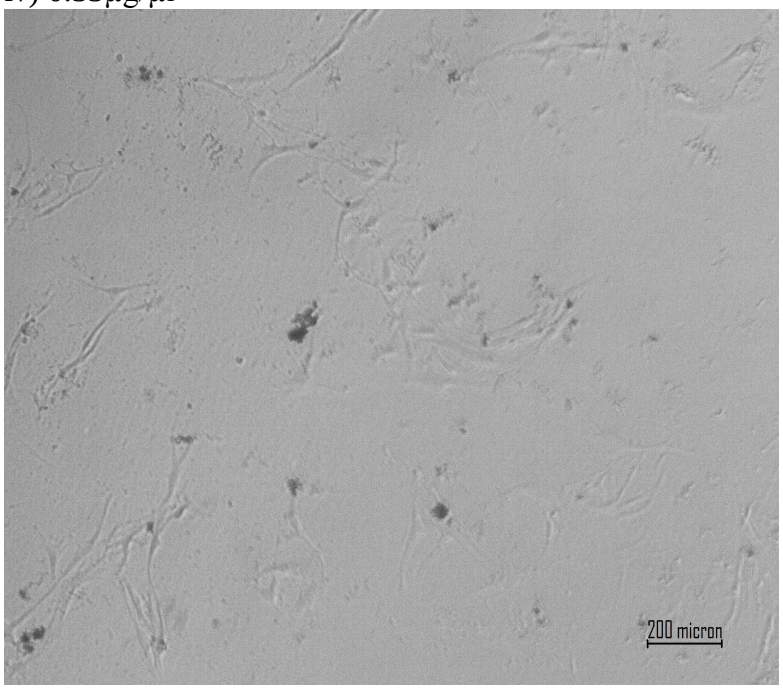

CHAPTER 5 DRUG RELEASE KINETICS

5.1 Loading and encapsulation studies

Camptothecin (CPT), an anticancer hydrophobic drug was used as the model drug. Loading and encapsulation efficiencies were calculated for the different polymeric ratios and the results were as shown. The DOB increase caused to decrease the size of the core of the particles which, in turn led to the decrease in loading capacity.[23]

Table 11: Loading efficiencies

Polymer	Loading efficiencies in %
Poly(EHMO-EHMO$_{PEG2000}$)$_{98.2:1.8}$	80
Poly(EHMO-EHMO$_{PEG2000}$)$_{96:4}$	73.8
Poly(EHMO-EHMO$_{PEG2000}$)$_{74.4:25.6}$	65
Poly(EHMO-EHMO$_{PEG550}$)$_{17:83}$	66

Table 12: Incorporation Efficiencies

Polymer	Incorporation Efficiency in %
Poly(EHMO-EHMO$_{PEG2000}$)$_{98.2:1.8}$	66
Poly(EHMO-EHMO$_{PEG2000}$)$_{96:4}$	65
Poly(EHMO-EHMO$_{PEG2000}$)$_{74.4:25.6}$	64
Poly(EHMO-EHMO$_{PEG550}$)$_{17:83}$	60

5.2 Drug release study

The drug release kinetics as shown in Figure 22, indicates that all poly(EHMO-EHMO$_{PEG}$) polymeric particles display a similar release pattern. A small burst effect takes place in the beginning between 1 to 20 hours and then a controlled and sustained release is observed. The order of release kinetics ranges from 0.3 to 0.7. The burst effect as observed in the beginning can be attributed to rapid diffusion of the drug that did not get trapped in the core. Therefore, the drug in the outer shell or on the surface released faster whereas, the core encapsulated drug releases at a much sustained manner. Since the drug used is a hydrophobic drug, hydrophobic interactions are the main reason for the controlled drug release. The release of the drug is also related to the degree of branching of the synthesized polymers. As indicated Figure 22, the release rate decreases with the increase in degree of branching. As the DOB increases, it causes more obstruction in the release of the drug and also causes the size of the particles to decrease as explained above. As a consequence the release rate also decreases. The release of the drug is mostly governed by diffusion of

water across the branched polymer. However, steric hindrance was also observed to have an influence over the drug release rate. The polymer with PEG_{550} (Poly(EHMO-$EHMO_{PEG})_{17:83}$) was found to have a higher release rate than the polymer with PEG_{2000} (Poly(EHMO-$EHMO_{PEG})_{74.4:25.6}$). This indicates that the drug release was slowed down by the presence of lengthier PEG chains.

Figure 22: Drug release kinetics

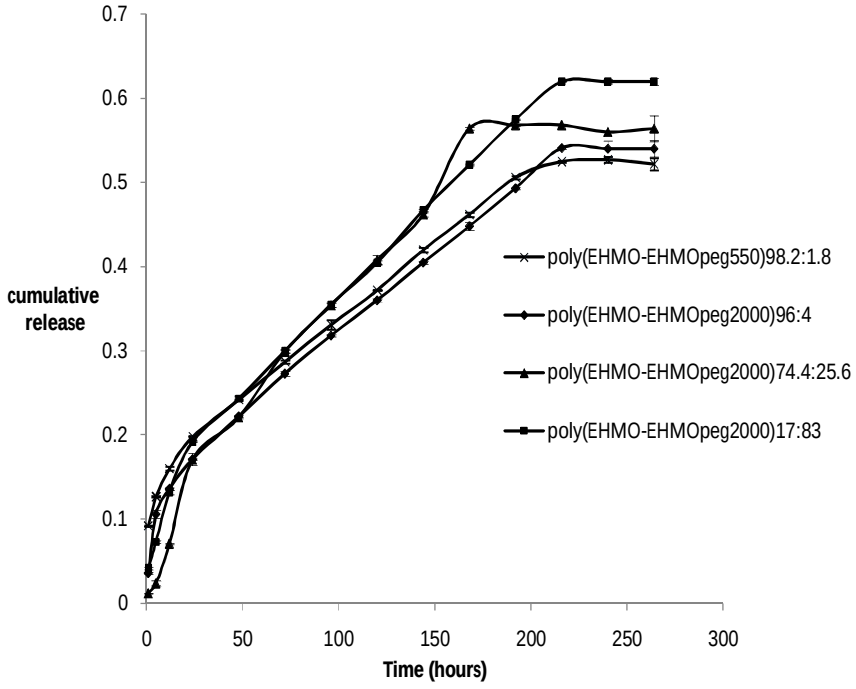

5.3 Cellular assay

Cellular assay was performed on HN12 cells to determine the efficacy of the encapsulated drug. MTT test conducted with 0.5µg/µl of concentration of poly(EHMO-$EHMO_{PEG2000}$)$_{74.4:25.6}$ showed that as the time increased from 12 to 72 hours the amount of cellular activity reduced indicating the release of drug from the particles as shown in Figure 23. The release was controlled and took place slowly over a period of time as indicated by the drug release studies. The percentage of the cellular activity became as low as 10% after 72 hours which indicated high potency of the drug.

Figure 23: Cellular assay

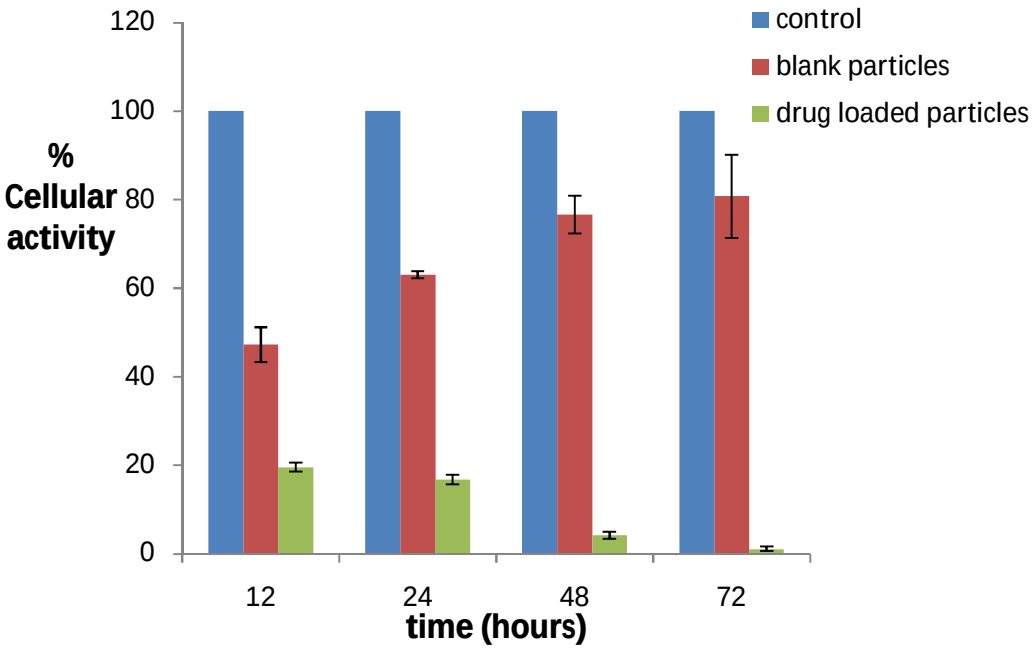

5.4 Conclusions

A new family of amphiphilic core-corona hyperbranched polymer, composed of EHMO and PEGylated EHMO was synthesized through cationic ring opening polymerization. It was characterized with NMR, FT-IR, DLS and DSC. Oil in water emulsion method was applied to formulate the synthesized polymers into particles for drug delivery.

Degree of branching was found to be dependent on the weight % ratio of EHMO/$EHMO_{PEG}$ and has a significant impact on polymeric properties including glass transition temperature, and drug loading efficiency. CPT can be released at a controlled and sustained rate. Addition of PEG chains to the polymer reduced the toxicity of the resulting hyperbranched polymer and made them more biocompatible.

CHAPTER 6 SUMMARY AND FUTURE WORK

Hyperbranched polymers have unique physical and chemical properties due to which they find potential applications in various fields including drug delivery to coatings.[26] They possess highly branched and three dimensional dendritic architecture, which makes them highly adaptable. We synthesized a novel amphiphilic polymeric system with potential for drug delivery and controlled release. We demonstrated the effect of addition of the monomer **2** (monomer with PEG chains) on the thermal properties, mechanical properties and drug release kinetics. We used Camptothecin, an anticancer hydrophobic drug for drug release studies; various other hydrophobic drugs can be used for future studies. All the studies done here were in vitro, therefore future studies must be done in vivo to get a better insight into how to utilize the synthesized polymeric system in human. Thermal analysis was done in this study to determine glass transition temperatures and its influence on the material. Further studies can be done to determine if the polymeric system shows any thermoresponsiveness.

Literature Cited

1. Vogelson, C. T., Advances in drug delivery. *Modern Drug Discovery* **2001,** Vol. 4,, (No. 4), 49-50, 52.
2. Gelperina, S.; Kisich, K.; Iseman, M. D.; Heifets, L., The potential advantages of nanoparticle drug delivery systems in chemotherapy of tuberculosis. *American Journal of Respiratory and Critical Care Medicine* **2005,** 172, (12), 1487-1490.
3. Tomalia, D. A., Birth of a new macromolecular architecture: dendrimers as quantized building blocks for nanoscale synthetic polymer chemistry. *Progress in Polymer Science* **2005,** 30, (3-4), 294-324.
4. Rosen, H.; Abribat, T., The rise and rise of drug delivery. *Nature Reviews Drug Discovery* **2005,** 4, (5), 381-385.
5. Irfan, M.; Seiler, M., Encapsulation Using Hyperbranched Polymers: From Research and Technologies to Emerging Applications. *Industrial & Engineering Chemistry Research* 49, (3), 1169-1196.
6. Holter, D.; Frey, H., Degree of branching in hyperbranched polymers .2. Enhancement of the DB: Scope and limitations. *Acta Polymerica* **1997,** 48, (8), 298-309.
7. Boas, U.; Christensen, J. B.; Heegaard, P. M. H., Dendrimers: design, synthesis and chemical properties. *Journal of Materials Chemistry* **2006,** 16, (38), 3786-3798.
8. DONALD A. TOMALIA, J. M. J. F. C., Discovery of Dendrimers and Dendritic Polymers:A Brief Historical Perspective*. *J. POLYM. SCI. PART A: POLYM. CHEM* **2002,** 40.
9. Worner, C.; Mulhaupt, R., Polynitrile-Functional and Polyamine-Functional Poly(Trimethylene Imine) Dendrimers. *Angewandte Chemie-International Edition in English* **1993,** 32, (9), 1306-1308.
10. Debrabandervandenberg, E. M. M.; Meijer, E. W., Poly(Propylene Imine) Dendrimers - Large-Scale Synthesis by Hetereogeneously Catalyzed Hydrogenations. *Angewandte Chemie-International Edition in English* **1993,** 32, (9), 1308-1311.
11. Tomalia, D. A.; Baker, H.; Dewald, J.; Hall, M.; Kallos, G.; Martin, S.; Roeck, J.; Ryder, J.; Smith, P., A New Class of Polymers - Starburst-Dendritic Macromolecules. *Polymer Journal* **1985,** 17, (1), 117-132.
12. Tomalia, D. A.; Baker, H.; Dewald, J.; Hall, M.; Kallos, G.; Martin, S.; Roeck, J.; Ryder, J.; Smith, P., Dendritic Macromolecules - Synthesis of Starburst Dendrimers. *Macromolecules* **1986,** 19, (9), 2466-2468.

13. Newkome, G. R.; Baker, G. R.; Arai, S.; Saunders, M. J.; Russo, P. S.; Theriot, K. J.; Moorefield, C. N.; Rogers, L. E.; Miller, J. E.; Lieux, T. R.; Murray, M. E.; Phillips, B.; Pascal, L., Cascade Molecules .6. Synthesis and Characterization of 2-Directional Cascade Molecules and Formation of Aqueous Gels. *Journal of the American Chemical Society* **1990,** 112, (23), 8458-8465.
14. Newkome, G. R.; Baker, G. R.; Saunders, M. J.; Russo, P. S.; Gupta, V. K.; Yao, Z. Q.; Miller, J. E.; Bouillion, K., 2-Directional Cascade Molecules - Synthesis and Characterization of [9]-N-[9] Arborols. *Journal of the Chemical Society-Chemical Communications* **1986**, (10), 752-753.
15. Grayson, S. M.; Frechet, J. M. J., Convergent dendrons and dendrimers: from synthesis to applications. *Chemical Reviews* **2001,** 101, (12), 3819-3867.
16. Donald A. Tomalia, J. M. J. F. C., A Brief Historical Perspective*.
17. Bosman, A. W.; Janssen, H. M.; Meijer, E. W., About dendrimers: Structure, physical properties, and applications. *Chemical Reviews* **1999,** 99, (7), 1665-1688.
18. Wooley, K. L.; Frechet, J. M. J.; Hawker, C. J., Influence of Shape on the Reactivity and Properties of Dendritic, Hyperbranched and Linear Aromatic Polyesters. *Polymer* **1994,** 35, (21), 4489-4495.
19. Hawker, C. J.; Farrington, P. J.; Mackay, M. E.; Wooley, K. L.; Frechet, J. M. J., Molecular Ball-Bearings - the Unusual Melt Viscosity Behavior of Dendritic Macromolecules. *Journal of the American Chemical Society* **1995,** 117, (15), 4409-4410.
20. Tomalia, D. A.; Hedstrand, D. M.; Ferritto, M. S., Comb-Burst Dendrimer Topology - New Macromolecular Architecture Derived from Dendritic Grafting. *Macromolecules* **1991,** 24, (6), 1435-1438.
21. Teertstra, S. J.; Gauthier, M., Dendrigraft polymers: macromolecular engineering on a mesoscopic scale. *Progress in Polymer Science* **2004,** 29, (4), 277-327.
22. Jikei, M.; Kakimoto, M., Hyperbranched polymers: a promising new class of materials. *Progress in Polymer Science* **2001,** 26, (8), 1233-1285.
23. Ajun, W.; Kou, Y. X., The characters of self-assembly core/shell nanoparticles of amphiphilic hyperbranched polyethers as drug carriers. *Journal of Nanoparticle Research* **2008,** 10, (3), 437-448.
24. Voit, B. I. L., A., Hyperbranched and Highly branched polymer architectures-synthetic stratergies and major characterization aspects. *Chem. Rev* **2009** 5924-5973.
25. Hult, A. M., E.; Magnusson, H. , Synthesis of hyperbranched aliphatic polyethers via cationic ring-opening polymerization of 3-ethyl-3-(hydroxyl)oxetane. *Macromol. Rapid Commun.* **1999**, 453-457.
26. Gao, C.; Yan, D., Hyperbranched polymers: from synthesis to applications. *Progress in Polymer Science* **2004,** 29, (3), 183-275.
27. Percec, V.; Kawasumi, M., Liquid-Crystalline Polyethers Based on Conformational Isomerism .23. Synthesis and Characterization of a Thermotropic Nematic Liquid-Crystalline Dendrimeric Polymer. *Macromolecules* **1992,** 25, (15), 3843-3850.

28. Percec, V.; Chu, P. W.; Kawasumi, M., Toward Willowlike Thermotropic Dendrimers. *Macromolecules* **1994,** 27, (16), 4441-4453.
29. Uhrich, K. E.; Hawker, C. J.; Frechet, J. M. J.; Turner, S. R., One-Pot Synthesis of Hyperbranched Polyethers. *Macromolecules* **1992,** 25, (18), 4583-4587.
30. Hawker, C. J.; Lee, R.; Frechet, J. M. J., One-Step Synthesis of Hyperbranched Dendritic Polyesters. *Journal of the American Chemical Society* **1991,** 113, (12), 4583-4588.
31. Bolton, D. H.; Wooley, K. L., Synthesis and characterization of hyperbranched polycarbonates. *Macromolecules* **1997,** 30, (7), 1890-1896.
32. Chang, H. T.; Frechet, J. M. J., Proton-transfer polymerization: A new approach to hyperbranched polymers. *Journal of the American Chemical Society* **1999,** 121, (10), 2313-2314.
33. Emrick, T.; Chang, H. T.; Frechet, J. M. J., An A(2)+B-3 approach to hyperbranched aliphatic polyethers containing chain end epoxy substituents. *Macromolecules* **1999,** 32, (19), 6380-6382.
34. Gong, C. G.; Frechet, J. M. J., Proton transfer polymerization in the preparation of hyperbranched polyesters with epoxide chain-ends and internal hydroxyl functionalities. *Macromolecules* **2000,** 33, (14), 4997-4999.
35. Holter, D.; Burgath, A.; Frey, H., Degree of branching in hyperbranched polymers. *Acta Polymerica* **1997,** 48, (1-2), 30-35.
36. Mai, Y. Y.; Zhou, Y. F.; Yan, D. Y.; Lu, H. W., Effect of reaction temperature on degree of branching in cationic polymerization of 3-ethyl-3-(hydroxymethyl)oxetane. *Macromolecules* **2003,** 36, (25), 9667-9669.
37. Zhu, Q.; Wu, J. L.; Tu, C. L.; Shi, Y. F.; He, L.; Wang, R. B.; Zhu, X. Y.; Yan, D. Y., Role of Branching Architecture on the Glass Transition of Hyperbranched Polyethers. *Journal of Physical Chemistry B* **2009,** 113, (17), 5777-5780.
38. Chanda, M., *Advanced Polymer Chemistry*. Marcel Dekker, Inc.: 2000; p 103-115.
39. Brigger, I.; Dubernet, C.; Couvreur, P., Nanoparticles in cancer therapy and diagnosis. *Advanced Drug Delivery Reviews* **2002,** 54, (5), 631-651.
40. Xu, J.; Zou, Y. F.; Pan, C. Y., Study on cationic ring-opening polymerization mechanism of 3-ethyl-3-hydroxymethyl oxetane. *Journal of Macromolecular Science-Pure and Applied Chemistry* **2002,** 39, (5), 431-445.
41. Bednarek, M.; Biedron, T.; Helinski, J.; Kaluzynski, K.; Kubisa, P.; Penczek, S., Branched polyether with multiple primary hydroxyl groups: polymerization of 3-ethyl-3-hydroxymethyloxetane. *Macromolecular Rapid Communications* **1999,** 20, (7), 369-372.
42. Mai, Y. Z., Y.; Yan, D., Synthesis and Size controllable self assembly of a novel amphiphilic hyperbranched multiarm copolether. *Macromolecules* **2005**, 8679-8686.
43. Sanna, N.; Chillemi, G.; Gontrani, L.; Grandi, A.; Mancini, G.; Castelli, S.; Zagotto, G.; Zazza, C.; Barone, V.; Desideri, A., UV-Vis Spectra of the Anticancer Campothecin Family Drugs in Aqueous Solution: Specific Spectroscopic

Signatures Unraveled by a Combined Computational and Experimental Study. *Journal of Physical Chemistry B* **2009,** 113, (16), 5369-5375.
44. Wall, M. E.; Wani, M. C.; Cook, C. E.; Palmer, K. H.; McPhail, A. T.; Sim, G. A., Plant Antitumor Agents .I. Isolation and Structure of Camptothecin a Novel Alkaloidal Leukemia and Tumor Inhibitor from Camptotheca Acuminata. *Journal of the American Chemical Society* **1966,** 88, (16), 3888-3890.
45. Bloomfield, V. A., Static and dynamic light scattering from aggregating particles. *Biopolymers* **2000,** 54, (3), 168-172.
46. Chen, L.; Tian, H. Y.; Chen, J.; Chen, X. S.; Huang, Y. B.; Jing, X. B., Multi-armed poly(L-glutamic acid)-graft-oligoethylenimine copolymers as efficient nonviral gene delivery vectors. *Journal of Gene Medicine* 12, (1), 64-76.
47. pecora, **B.** j. b. R., *Dynamic light scattering with applications to chemistry, biology and physics*. Dover publications, Inc.: **2000**; p 3-10.
48. Grcev, S.; Schoenmakers, P.; Iedema, P., Determination of molecular weight and size distribution and branching characteristics of PVAc by means of size exclusion chromatography/multi- angle laser light scattering (SEC/MALLS). *Polymer* **2004,** 45, (1), 39-48.
49. Postek, M. T., Handbook of Charged Particle Optics. In Orloff, J., Ed. CRC press LLC: 1997; pp 363-367.
50. Dou, H. J.; Tang, M. H.; Yang, W. H.; Sun, K., One-pot synthesis, characterization, and drug loading of polysaccharide-based nanoparticles with carboxy functional groups. *Colloid and Polymer Science* **2007,** 285, (9), 1043-1047.

VITA

Khushboo Sharma is a resident of Uttar Pradesh, India. Khushboo completed her undergraduate degree in Biotechnology Engineering from ICFAI Institute of Science and Technology in 2008. She began her graduate studies in Biomedical Engineering at Virginia Commonwealth University in fall 2008. Khushboo is very keen on expanding her knowledge in a field combining medicine and engineering. She has taken admission into the Ph.D. program in Biomedical Sciences Department at VCU School of Medicine from fall 2010.